(12) INTERNATIONAL APPLICATION PUBLISHED UNDER THE PATENT COOPERATION TREATY (PCT)

(19) World Intellectual Property Organization
International Bureau

(43) International Publication Date
16 December 2004 (16.12.2004)

PCT

(10) International Publication Number
WO 2004/108074 A2

(51) International Patent Classification[7]: A61K

(21) International Application Number: PCT/US2004/015244

(22) International Filing Date: 14 May 2004 (14.05.2004)

(25) Filing Language: English

(26) Publication Language: English

(30) Priority Data:
60/476,209 5 June 2003 (05.06.2003) US

(71) Applicant: RESEARCH DEVELOPMENT FOUNDATION [US/US]; 402 North Division Street, Carson City, NV 89703 (US).

(72) Inventor: ROSENBLUM, Michael; 3127 Stoney Mist Dirve, Sugarland, TX 77479 (US).

(74) Agent: ADLER, Benjamin, A.; Adler & Associated, 8011 Candle Lane, Houston, TX 77071 (US).

(81) Designated States *(unless otherwise indicated, for every kind of national protection available)*: AE, AG, AL, AM, AT, AU, AZ, BA, BB, BG, BR, BW, BY, BZ, CA, CH, CN, CO, CR, CU, CZ, DE, DK, DM, DZ, EC, EE, EG, ES, FI, GB, GD, GE, GH, GM, HR, HU, ID, IL, IN, IS, JP, KE, KG, KP, KR, KZ, LC, LK, LR, LS, LT, LU, LV, MA, MD, MG, MK, MN, MW, MX, MZ, NA, NI, NO, NZ, OM, PG, PH, PL, PT, RO, RU, SC, SD, SE, SG, SK, SL, SY, TJ, TM, TN, TR, TT, TZ, UA, UG, US, UZ, VC, VN, YU, ZA, ZM, ZW.

(84) Designated States *(unless otherwise indicated, for every kind of regional protection available)*: ARIPO (BW, GH, GM, KE, LS, MW, MZ, NA, SD, SL, SZ, TZ, UG, ZM, ZW), Eurasian (AM, AZ, BY, KG, KZ, MD, RU, TJ, TM), European (AT, BE, BG, CH, CY, CZ, DE, DK, EE, ES, FI, FR, GB, GR, HU, IE, IT, LU, MC, NL, PL, PT, RO, SE, SI, SK, TR), OAPI (BF, BJ, CF, CG, CI, CM, GA, GN, GQ, GW, ML, MR, NE, SN, TD, TG).

Published:
— *without international search report and to be republished upon receipt of that report*

For two-letter codes and other abbreviations, refer to the "Guidance Notes on Codes and Abbreviations" appearing at the beginning of each regular issue of the PCT Gazette.

WO 2004/108074 A2

(54) Title: VASCULAR ENDOTHELIAL GROWTH FACTOR FUSION CONSTRUCTS AND USES THEREOF

(57) Abstract: The 121-amino acid isoform of vascular endothelial growth factor ($VEGF_{121}$) is linked by a flexible G4S tether to a cytotoxic molecule such as toxin gelonin or granzyme B and expressed as a soluble fusion protein. The $VEGF_{121}$ fusion protein exhibits significant anti-tumor vascular-ablative effects that inhibit the growth of primary tumors and inhibit metastatic spread and vascularization of metastases. The $VEGF_{121}$ fusion protein may also target osteoclast precursor cells *in vivo* and inhibits osteoclastogenesis.

VASCULAR ENDOTHELIAL GROWTH FACTOR FUSION CONSTRUCTS AND USES THEREOF

BACKGROUND OF THE INVENTION

Field of the Invention

The present invention relates generally to the fields of cancer research and targeted therapy. More specifically, the present invention relates to fusion constructs comprising the 121-amino acid isoform of vascular endothelial growth factor ($VEGF_{121}$) and uses of such contructs.

Description of the Related Art

Vascular endothelial growth factor (VEGF)-A plays a central role in the growth and metastasis of solid tumors, and acts as a primary stimulant of vascularization in solid tumors. VEGF-A enhances endothelial cell proliferation, migration, and survival and is essential for blood vessel formation. Other roles of vascular endothelial growth factor include wound healing, vascular permeability and the regulation of blood flow. Through alternative splicing of RNA, human vascular endothelial growth factor exists as at least four isoforms of 121, 165, 189, or 206 amino acids. The lowest molecular weight isoform, designated $VEGF_{121}$, is a non-heparan sulfate-binding isoform that exists in solution as a disulfide-linked homodimer.

VEGF is released by a variety of tumor cells. The angiogenic actions of VEGF are mediated through two related receptor tyrosine kinases, kinase domain receptor (KDR) and FLT-1 in the human, and Flk-1 and Flt-1 in the mouse. Both are largely restricted to vascular endothelial cells. KDR/Flk-1 and FLT-1 receptors are overexpressed on the endothelium of tumor vasculature. In contrast, these receptors

are almost undetectable in the vascular endothelium of adjacent normal tissues. The receptors for vascular endothelial growth factor thus seem to be excellent targets for the development of therapeutic agents that inhibit tumor growth and metastatic spread through inhibition of tumor neovascularization.

To this end, $VEGF_{121}$ would be an appropriate carrier to deliver a toxic agent selectively to tumor vascular endothelium. $VEGF_{121}$ exists in solution as a disulfide linked homodimer and binds to KDR and FLT-1 in a heparin-independent manner. It does not bind neuropilin-1 or neuropilin-2. $VEGF_{121}$ has been shown to contain the full biological activity of the larger variants.

Molecular engineering enabled the synthesis of novel chimeric molecules having therapeutic potential. Chimeric fusion constructs targeting the IL-2 receptor, the EGF receptor, and other growth factor/cytokine receptors have been described. It has also been showed that a chemical conjugate of vascular endothelial growth factor and truncated diphtheria toxin has impressive cytotoxic activity on cell lines expressing receptors for vascular endothelial growth factor. Further studies with VEGF/diphtheria toxin fusion constructs demonstrated selective toxicity to Caprice's sarcoma cells and dividing endothelial cells *in vitro* and *in vivo*. However, the prior art is deficient in fusion constructs comprising vascular endothelial growth factor and other cytotoxic molecule with improved biochemical and pharmacological properties. The present invention fulfills this long-standing need and desire in the art.

SUMMARY OF THE INVENTION

The present invention discloses targeting of neovasculature of solid tumors with a chimeric fusion toxin comprising the 121-amino acid isoform of vascular endothelial growth factor ($VEGF_{121}$). In one embodiment, the chimeric fusion toxin ($VEGF_{121}$/rGel) consists of $VEGF_{121}$ and recombinant gelonin (rGel), a low molecular weight single chain toxin with a mechanism of action similar to that of ricin A-chain. $VEGF_{121}$ is linked by a flexible G4S tether to the toxin gelonin and expressed as a soluble protein in bacteria. Both $VEGF_{121}$/rGel and $VEGF_{121}$ stimulated cellular kinase domain receptor (KDR) phosphorylation. The $VEGF_{121}$/rGel fusion construct was highly cytotoxic to endothelial cells overexpressing the KDR/Flk-1 receptor.

Endothelial cells overexpressing FLT-1 were not sensitive to the fusion protein.

While several studies have shown both receptors of $VEGF_{121}$, namely VEGFR-1 (FLT-1) and VEGFR-2 (KDR/Flk-1), to be over-expressed on the endothelium of tumor vasculature, the present invention reports several surprising results which demonstrate that $VEGF_{121}$/rGel has several advantageous properties. Cell ELISA using antibodies specific to either KDR or FLT-1 indicate binding of $VEGF_{121}$/rGel to both receptors. While $VEGF_{121}$/rGel binds to both FLT-1 and KDR, internalization of $VEGF_{121}$/rGel is mediated only by KDR and not FLT-1.

Experiments with human melanoma (A-375) or human prostate (PC-3) xenografts demonstrate successful use of $VEGF_{121}$/rGel fusion construct for the targeted destruction of tumor vasculature *in vivo*. The present invention also indicates that the anti-tumor vascular-ablative effect of $VEGF_{121}$/rGel may be utilized not only for treating primary tumors but also for inhibiting metastatic spread and vascularization of metastases. Taken together, these results indicate that selective destruction of tumor vasculature can be achieved with $VEGF_{121}$/rGel in mice, giving impressive antitumor effects. Gross morphological toxicity to normal organs was not visible in animals treated with a therapeutic dose. Therefore, $VEGF_{121}$/rGel is a potential antitumor agent useful for treating cancer patients.

In another embodiment of the present invention, there is provided a chimeric fusion toxin (GrB/$VEGF_{121}$) consists of $VEGF_{121}$ and granzyme B (GrB), a serine protease capable of inducing apoptosis through both caspase-dependent and caspase-independent pathways. GrB/$VEGF_{121}$ induced apoptotic events specifically on FLK-1-expressing porcine aortic endothelial cells as assessed by terminal deoxynucleotidyl transferase-mediated nick end labeling assay, DNA laddering, and cytochrome c release from mitochondria. In addition, the fusion construct mediated cleavage of caspase-8, caspase-3, and poly(ADP-ribose) polymerase in target endothelial cells within 4 h after treatment. In conclusion, delivery of the human proapoptotic pathway enzyme granzyme B to tumor vascular endothelial cells or to tumor cells may have significant therapeutic potential and represents a potent new class of targeted therapeutic agents with a unique mechanism of action.

The present invention is directed to a composition of matter comprising a conjugate comprising the 121-amino acid isoform of vascular endothelial

growth factor ($VEGF_{121}$) and a cytotoxic molecule. In general, the cytotoxic molecule is a toxin such as gelonin or a molecule that induces apoptosis such as granzyme B.

In another embodiment of the present invention, there is provided a method of using the $VEGF_{121}$ fusion conjugate of the present invention to kill cells expressing type 2 VEGF receptors (kinase domain receptor/Flk-1 receptors). The $VEGF_{121}$ component of the conjugate binds to both VEGF receptor type 1 (Flt-1) and VEGF receptor type 2 (KDR/Flk-1) but is only internalized by cells expressing VEGF receptor type 2.

In yet another embodiment of the present invention, there is provided a method of using the $VEGF_{121}$ fusion conjugate of the present invention to inhibit tumor growth or inhibit metastatic spread and vascularization of metastases in an animal or a human.

The present invention further provides a method of using the $VEGF_{121}$ fusion conjugate of the present invention to inhibit osteoclastogenesis or treat osteoporosis in an animal or a human.

Other aspects, features, and advantages of the present invention will be apparent from the following description of the presently preferred embodiments of the invention. These embodiments are given for the purpose of disclosure.

BRIEF DESCRIPTION OF THE DRAWINGS

Figure 1 shows the design and construction of $VEGF_{121}$/rGel. Constructs of the targeting molecule ($VEGF_{121}$) to the cytotoxic agent (gelonin) were expressed in two orientations, with either $VEGF_{121}$ or gelonin at the N-terminus. A G4S tether was used to fuse $VEGF_{121}$ and gelonin and reduce steric hindrance.

Figure 2 shows a rabbit reticulocyte assay used to determine the ability of $VEGF_{121}$/rGel and rGel to inhibit translation in a cell-free system. The fusion of $VEGF_{121}$ and recombinant gelonin does not reduce the activity of the toxin component.

Figure 3 shows an ELISA demonstrating that $VEGF_{121}$/rGel binds to the receptor. $VEGF_{121}$/rGel, $VEGF_{121}$ and rGel were incubated with biotinylated

mouse flk-1 receptor attached to NeutrAvidin-coated plates. Binding was assessed using anti-gelonin and anti-VEGF antibodies.

Figure 4 shows binding to flk-1 receptor is specific for $VEGF_{121}$/rGel. $VEGF_{121}$/rGel or $VEGF_{121}$ was incubated with flk-1 receptor. Binding of $VEGF_{121}$/rGel was competed with $VEGF_{121}$ and a rabbit anti-gelonin antibody was used for detection. $VEGF_{121}$ specifically reduced binding of $VEGF_{121}$/rGel to flk-1. $VEGF_{121}$ was not detected by the anti-gelonin antibody (data not shown).

Figure 5 shows cytotoxicity of $VEGF_{121}$/rGel to KDR-expressing porcine aortic endothelial cells (PAE). Cells transfected with either the FLT-1 or KDR receptor were treated with various doses of $VEGF_{121}$/rGel or rGel for 72 h. Cells expressing the FLT-1 receptor were equally insensitive to $VEGF_{121}$/rGel and rGel (IC_{50}/300 nM). In contrast, cells expressing KDR were about 200-fold more sensitive to the fusion construct (IC_{50} of 0.5 nM) than they were to rGel.

Figures 6A-B show expression of KDR and FLT-1. Figure 6A: Whole cell lysate (30 μg) of PAE/KDR and PAE/FLT-1 was run on an SDS-PAGE gel, transferred to a PVDF membrane and immunoblotted using the appropriate antibody. Expression of both receptors on their respective cell lines was confirmed. Figure 6B: Receptor-specific binding of radio-labeled $VEGF_{121}$/rGel is demonstrated on cells expressing these receptors. Binding was reduced with unlabeled $VEGF_{121}$/rGel but not by unlabeled gelonin.

Figure 7 shows internalization of $VEGF_{121}$/rGel into PAE/KDR and PAE/FLT-1 cells. PAE/KDR cells were incubated with 4 μg/ml $VEGF_{121}$/rGel at the timepoints indicated. Cells were then incubated with an anti-gelonin polyclonal antibody (1:200) followed by a FITC-conjugated secondary antibody (1:80). Nuclei were stained with propidium iodide. $VEGF_{121}$/rGel enters PAE/KDR cells within one hour of treatment. However, PAE/FLT-1 cells did not internalize $VEGF_{121}$/rGel even after 24 hours of incubation with $VEGF_{121}$/rGel.

Figure 8 shows the effect of exposure time of $VEGF_{121}$/rGel on PAE/KDR cells on cytotoxicity. $VEGF_{121}$/rGel was incubated with PAE/KDR cells for varying lengths of time. While $VEGF_{121}$/rGel retained cytotoxicity towards PAE/KDR cells even with a 1 h exposure time, cytotoxicity of this fusion toxin was markedly enhanced by an exposure time of 48 hours.

Figure 9 shows that cytotoxicity of $VEGF_{121}$/rGel to PAE/KDR cells does not result in apoptosis. PAE/KDR cells were grown overnight. 1 nM $VEGF_{121}$/rGel (twice the IC_{50}) was added and incubated for 24, 48 and 72 hours. The cells were analyzed for TUNEL. Positive control cells were incubated with 1 mg/ml DNAse for 10 minutes at 37°C.

Figure 10 shows that treatment of PAE/KDR cells with $VEGF_{121}$/rGel does not result in PARP cleavage. PAE/KDR cells were stimulated with $VEGF_{121}$/rGel or $VEGF_{121}$ for the times indicated. Cells were washed and lysed and the cell lysate was analyzed by Western using an anti-PARP antibody. No PARP cleavage was observed.

Figure 11 shows inhibition of human melanoma growth in mice by VEGF/rGel. Groups of nude mice bearing A-375M tumors were treated intravenously with saline, rGel, or fusion construct every 2–3 days for 11 days. Administration of rGel did not affect tumor growth. Treatment with $VEGF_{121}$/rGel at a total dose of either 17 mg/kg or 25 mg/kg significantly suppressed tumor growth. However, treatment at the 25 mg/kg dose level resulted in mortality by day 19. None of the animals dosed at 17 mg/kg showed gross evidence of toxicity.

Figure 12 shows inhibition of human prostate carcinoma growth in mice by VEGF/rGel. Groups of nude mice bearing PC-3 tumors were treated intravenously with saline, rGel, or the $VEGF_{121}$/rGel fusion construct (20 mg/kg total dose) every 2–3 days for 11 days. Administration of rGel (10 mg/kg) had no effect on tumor growth. In contrast, treatment with the fusion construct completely inhibited tumor growth for 26 days and resulted in a 7-fold reduction in tumor volume compared with saline-treated or rGel-treated controls.

Figure 13 shows the specific localization of VEGF/rGel to tumor vasculature in PC3 tumors. Nude mice bearing human prostate PC-3 tumors were injected i.v. with $VEGF_{121}$/rGel or rGel (2.5 mg/kg). Thirty minutes after administration, tissues were removed and snap frozen. Sections were stained with immunofluorescent reagents to detect murine blood vessels (MECA-32, red) and with antirGel (green). Vessels stained with both reagents appear yellow. VEGF/rGel localized to tumor vessels, whereas rGel did not. Vessels in all normal organs other than the kidney (glomerulus) were unstained by VEGF/rGel.

Figure 14 shows the destruction and thrombosis of tumor blood vessels by VEGF/rGel. Nude mice bearing human prostate PC-3 tumors were treated i.v. with one dose of $VEGF_{121}$/rGel (2.5 mg/kg). Forty-eight hours after administration, tissues were snap-frozen, sectioned, and stained with hematoxylin and eosin. As shown in this representative image, tumors from mice treated with the fusion construct had damaged vascular endothelium. Clots were visible in the larger vessels of the tumors, and erythrocytes were visible in the tumor interstitium, indicating a loss of vascular integrity. In contrast, histological damage was not visible in any normal organs, including the kidneys, of treated mice.

Figures 15A-B show $VEGF_{121}$/rGel is not cytotoxic to MDA-MB-231 cells. Log-phase MDA-MB-231 cells were treated with various doses of $VEGF_{121}$/rGel or rGel for 72 hrs. The cytotoxic effects of both agents were similar, indicating no specific cytotoxicity of the fusion construct compared to free toxin on these cells (Figure 15B). Western analysis demonstrated the presence of VEGFR-2 on endothelial cells transfected with the R2 receptor (PAE/KDR) but not on cells expressing the FLT-1 receptor (PAE/FLT-1, negative control). The MDA-MB-231 cells did not express detectable amounts of VEGFR-2 (Figure 15A).

Figure 16 shows $VEGF_{121}$/rGel localizes to blood vessels of MDA-MB-231 tumor. Mice bearing orthotopically-placed MDA-MB-31 tumors were administered one dose (i.v., tail vein) of $VEGF_{121}$/rGel. Four hours later, the mice were sacrificed and tumors excised and fixed. Tissue sections were stained for blood vessels using the Meca 32 antibody (red) and the section was counter-stained using an anti-gelonin antibody (green). Co-localization of the stains (yellow) demonstrate the presence of the $VEGF_{121}$/rGel fusion construct specifically in blood vessels and not on tumor cells.

Figure 17 shows $VEGF_{121}$/rGel reduces number of large metastatic colonies in lungs. The size of tumor colonies was analyzed on slides stained with 6w/32 antibody that specifically recognizes human HLA antigens. The antibody delineates colonies of human tumor cells and defines borders between metastatic lesions and mouse lung parenchyma. The largest size differences between $VEGF_{121}$/rGel and control groups were found in groups of colonies having diameter either less than 50 μm or more than 1000 μm. In the $VEGF_{121}$/rGel-treated mice more

than 40% of total foci were extremely small (< 50 micron) as compared to 18% in the control group. The control mice had approximately 8% of extremely large colonies (>1000 μm) whereas $VEGF_{121}$/rGel-treated mice did not have colonies of this size.

Figures 18A-B show $VEGF_{121}$/rGel inhibits vascularization of MDA-MB-231 pulmonary metastases. Lungs derived from $VEGF_{121}$/rGel and rGel - treated mice were stained with MECA 32 antibody and the number of vessels per mm^2 within the metastatic foci was determined (Figure 18A). The mean number of vessels per mm^2 in lung metastases of $VEGF_{121}$/rGel-treated mice was reduced by approximately 50% as compared to those in rGel-treated mice. Figure 18B shows representative images demonstrating reduction of vascular density in foci of comparable size in mice treated with rGel (left) and $VEGF_{121}$/rGel fusion protein (right).

Figure 19 shows $VEGF_{121}$/rGel inhibits proliferation of metastatic MDA-MB-231 cells in the lungs. Frozen sections of lungs derived from $VEGF_{121}$/rGel or rGel-treated mice were stained with Ki-67 antibody. Stained sections were examined under x40 objective to determine the number of tumor cells with positive nuclei (cycling cells). Positive cells were enumerated in 10 colonies per slide on six sections derived from individual mice per each treatment group. The mean number per group ± SEM is presented. $VEGF_{121}$/rGel treatment reduced the average number of cycling cells within the metastatic foci by approximately 60%.

Figure 20 shows detection of VEGFR-2 on vasculature of metastatic lesions by anti-VEGFR-2 antibody RAFL-1. Frozen sections of lungs from mice treated with $VEGF_{121}$/rGel or free gelonin were stained with monoclonal rat anti-mouse VEGFR-2 antibody RAFL-1 (10 μg/ml). RAFL-1 antibody was detected by goat anti-rat IgG-HRP. Sections were developed with DAB and counterstained with hematoxylin. Representative images of lung metastases of comparable size (700-800 μm in the largest diameter) from each treatment group are shown. Images were taken with an objective of X20. Note that the pulmonary metastases from the $VEGF_{121}$/rGel treated group show both reduced vessel density and decreased intensity of anti-VEGFR-2 staining compared to control lesions.

Figure 21 shows $VEGF_{121}$/rGel strongly inhibits the growth of prostate cancer cells PC-3 placed in the bone micro-environment in mice. Animals were anesthesized prior to injection of 50,000 PC-3 cells into the distal epipysis of

the right femur. Treatment with $VEGF_{121}$/rGel or saline (control) began one week after tumor placement. The maximum tolerated dose of $VEGF_{121}$/rGel was utilized and administered i.v. as shown. Tumor growth was monitored by X-ray and animals with large osteolytic lesions or bone lysis were sacrificed. All control mice were sacrificed by day 67. In contrast, 50% of the $VEGF_{121}$/rGel-treated mice survived past day 140 without sign of osteolysis.

Figure 22 shows the effects of $VEGF_{121}$/rGel and rGel on RANKL-mediated osteoclast formation. Raw 264.7 cells were cultured overnight in 24-well plates. Osteoclast formation was induced by addition of 100 ng/ml RANKL with increasing concentrations of $VEGF_{121}$/rGel or rGel. Cells were allowed to differentiate for 96 hours followed by determination of the number of osteoclasts per well. Each experiment was performed in triplicate. The data shown is representative of three separate experiments. RANKL or RANKL + rGel-treated Raw 264.7 cells differentiate into large multi-nucleated TRAP-positive osteoclasts. In contrast, RANKL + $VEGF_{121}$/rGel-treated cells do not differentiate and do not stain for TRAP.

Figure 23 shows cloning of human granzyme B (GrB) gene from HuT-78 cells. HuT-78 RNA was isolated, and premature GrB cDNA (~800 bp) was amplified by reverse transcription-PCR and cloned into the PCR 2.1 TA vector. The human granzyme B sequence with 20-amino acid signal sequence was confirmed and designated as premature granzyme B. Once the signal peptide was removed, the mature amino-terminal Ile-Ile-Gly-Gly sequence of granzyme B was generated.

Figure 24 shows the construction of GrB/$VEGF_{121}$ fusion toxin by PCR and insertion into the pET32a(+) vector. Mature granzyme B was attached to the recombinant $VEGF_{121}$ carrier via a flexible tether (G4S). A cleavage site for EK (DDDDK) was inserted upstream and adjacent to the first amino acid isoleucine of granzyme B. The fused gene fragment was then introduced into *Xba*I and *Xho*I sites of the pET32a(+) vector to form the expression vector pET32GrB/$VEGF_{121}$.

Figures 25A-B show bacterial expression, purification, and Western blot analysis of the GrB/$VEGF_{121}$ fusion toxin. Figure 25A: 8.5% SDS-PAGE and Coomassie blue staining under reducing conditions showed that GrB/$VEGF_{121}$ was expressed as a 55-kDa molecule with tags and the size of the final purified GrB/$VEGF_{121}$ was ~38 kDa. Figure 25B: Western blotting confirmed that the fusion

protein reacted with either mouse anti-VEGF or mouse anti-GrB antibody.

Figures 26A-B show GrB/$VEGF_{121}$ bound to PAE/FLK-1 cells but not to PAE/FLT-1 cells, A375M or SKBR3 cells. Binding of GrB/$VEGF_{121}$ to cells was assessed by 96-well ELISA plates coated with 50,000 cells/well of PAE/FLK-1, PAE/FLT-1, A375M or SKBR3 cells. The wells were blocked with 5% BSA and then treated with purified GrB/$VEGF_{121}$ at various concentrations. The wells were then incubated with either anti-GrB antibody (Figure 26A) or anti-VEGF antibody (Figure 26B) followed by HRP-goat anti-mouse IgG. ABTS solution with 1 ml/ml of 30% H_2O_2 were added to the wells, and absorbance at 405 nm was measured after 30 min.

Figure 27 shows internalization of GrB/$VEGF_{121}$ into porcine aortic endothelial (PAE) cells. PAE cells were plated onto 16-well chamber slides (1 x 10^4 cells/well), treated with 100 nM of GrB/$VEGF_{121}$ for 4 h and then washed briefly with PBS. The cell surface was stripped with glycine buffer (pH 2.5) and the cells were fixed in 3.7% formaldehyde and permeabilized in PBS containing 0.2% Triton X-100. After blocking, samples were incubated with anti-granzyme B antibody and treated with FITC-coupled anti-mouse IgG. The slides were analyzed under a fluorescence microscope. The granzyme B moiety of GrB/$VEGF_{121}$ was delivered into the cytosol of PAE/FLK-1 but not into that of PAE/FLT-1 cells after 4-h treatment.

Figure 28A shows cytotoxicity of the GrB/$VEGF_{121}$ fusion toxin on transfected endothelial cells. Log-phase PAE cells were plated into 96-well plates at a density of 2.5 x 10^3 cells/well and allowed to attach for 24 h. The medium was replaced with medium containing different concentrations of GrB/$VEGF_{121}$. After 72 h, the effect of fusiontoxin on the growth of cells in culture was determined using XTT. Plates were read on a microplate ELISA reader at 540 nm. IC_{50} of GrB/$VEGF_{121}$ was ~10 nM on PAE/FLK-1 cells; it was not cytotoxic on PAE/FLT-1 cells.

Figure 28B shows growth inhibitory effects of GrB/$VEGF_{121}$ as determined by colony-forming assay. PAE cells (5 x 10^5 cells/ml) were incubated at 37^0C and 5% CO_2 for 72 h with different concentrations of GrB/$VEGF_{121}$ and 100 nM of irrelevant fusion protein GrB/scFvMEL. Cells were then washed with PBS, trypsinized, counted, and diluted serially. The serial cell suspensions were then

plated in triplicate and cultured in six-well plates for 5–7 days. Cells were stained with crystal violet and colonies consisting of >20 cells were counted. The results are shown as percentage of colonies in relation to the number of colonies formed by untreated cells.

Figures 29A-B show GrB/$VEGF_{121}$ induces apoptosis on PAE/FLK-1 cells. Cells ($1x10^4$ cells/well) were treated with GrB/$VEGF_{121}$ at an IC_{50} concentration for different times (0, 24, and 48 h) and washed with PBS. Cells were fixed with 3.7% formaldehyde and permeabilized with 0.1% Triton X-100 and 0.1% sodium citrate. Cells were incubated with TUNEL reaction mixture, incubated with Converter-AP, and finally treated with Fast Red substrate solution. The slides were analyzed under a light microscope. Apoptosis cells were stained red (400x) (Figure 29A). Figure 29B shows apoptotic cells as percentage of the total counted cells (>200 cells) in randomly selected fields (200x); bars, SD.

Figure 30 shows granzyme B/$VEGF_{121}$ induces cytochrome c release from mitochondria to cytosol and Bax translocation from cytosol to mitochondria. PAE cells (5×10^7) were treated with granzyme B/$VEGF_{121}$ at concentrations of 0, 0.1, and 20 nM for 24 h. Cells were collected, and the cytosolic and mitochondrial fractions were isolated as described below. Fractions of 30 mg each from non-treated and treated cells were loaded onto 15% SDS-PAGE gels, and standard Western blotting procedure was performed. The blot was probed with anti-cytochrome c antibody or anti-Bax antibody.

Figure 31 shows GrB/$VEGF_{121}$ induces DNA laddering in PAE/FLK-1 cells. Cells were plated into six-well plates at a density of 2×10^5 cells/well and exposed to 20 nM GrB/$VEGF_{121}$ for 24 h. DNA was isolated from cell lysates and fractionated on 1.5% agarose gel.

Figure 32 shows cleavage and activation of caspase-3, caspase-8, and PARP in PAE/FLK-1 cells treated with GrB/$VEGF_{121}$. PAE cells were plated into six-well plates at a density of 2×10^5 cells/well and treated with 20 nM GrB/$VEGF_{121}$ for 4 h. The total cell lysates were loaded onto 12% SDS-PAGE and Western blot was performed using appropriate primary antibodies.

DETAILED DESCRIPTION OF THE INVENTION

The expression of vascular endothelial growth factor and its receptors has been closely linked to tumor vascularity, metastasis, and progression. Several groups have developed anti-angiogenic drugs that block kinase activity of the vascular endothelial growth factor receptors or monoclonal antibodies that block vascular endothelial growth factor–receptor interactions. The present invention demonstrates chimeric fusion constructs containing the 121-amino acid isoform of vascular endothelial growth factor ($VEGF_{121}$) and a cytotoxic molecule such as plant toxin gelonin or serine protease granzyme B.

Agents targeting the neovascularization process in tumors have significant potential for therapeutic impact. Molecules which interfere with the growth and development of vascular endothelial cells by targeting the VEGF/receptor complex have an additional advantage since these agents do not have to penetrate into the tumor parenchyma and the receptor targets are expressed on the luminal surface of tumor vascular endothelium.

Possible binding of vascular endothelial growth factor-containing constructs to the neuropilin receptor could be a source of unwanted toxicity and mis-targeting of the complex; however, it has been shown that the $VEGF_{121}$ fragment as opposed to other isoforms of VEGF-A does not appear to bind to this receptor.

It is specifically contemplated that pharmaceutical compositions may be prepared using the novel fusion constructs of the present invention. In such a case, the pharmaceutical composition comprises the novel fusion constructof the present invention and a pharmaceutically acceptable carrier. A person having ordinary skill in this art would readily be able to determine, without undue experimentation, the appropriate dosages and routes of administration of this fusion toxin of the present invention. When used *in vivo* for therapy, the fusion construct of the present invention is administered to the patient or an animal in therapeutically effective amounts, i.e., amounts that eliminate or reduce the tumor burden or other desired biological effects. It will normally be administered parenterally, preferably intravenously, but other routes of administration will be used as appropriate.

The dose and dosage regimen will depend upon the nature of the disease or cancer (primary or metastatic) and its population, the characteristics of the particular fusion toxin, *e.g.*, its therapeutic index, the patient, the patient's history and other factors. The amount of fusion toxin administered will typically be in the range of about 0.01 to about 100 mg/kg of patient weight. The schedule will be continued to optimize effectiveness while balanced against negative effects of treatment. *See Remington's Pharmaceutical Science*, 17th Ed. (1990) Mark Publishing Co., Easton, Penn.; and *Goodman and Gilman's: The Pharmacological Basis of Therapeutics*, 8th Ed. (1990) Pergamon Press. For parenteral administration, the fusion toxin protein will most typically be formulated in a unit dosage injectable form (solution, suspension, emulsion) in association with a pharmaceutically acceptable parenteral vehicle. Such vehicles are preferably non–toxic and non–therapeutic. Examples of such vehicles are water, saline, Ringer's solution, dextrose solution, and 5% human serum albumin. Nonaqueous vehicles such as fixed oils and ethyl oleate may also be used.

Liposomes may be used as carriers. The vehicle may contain minor amounts of additives such as substances that enhance isotonicity and chemical stability, *e.g.*, buffers and preservatives. The fusion toxin will typically be formulated in such vehicles at concentrations of about 0.01 mg/ml to 1000 mg/ml.

As used herein, a "subject" refers to an animal or a human.

The present invention is directed to a composition of matter comprising a conjugate comprising the 121-amino acid isoform of vascular endothelial growth factor ($VEGF_{121}$) and a cytotoxic molecule. In general, the cytotoxic molecule is a toxin such as gelonin or a signal transduction protein capable of generating apoptotic signals. Representative useful signal transduction proteins include granzyme B and Bax. In one embodiment, the conjugate is a fusion protein in which $VEGF_{121}$ and the cytotoxic molecule are linked by a linker such as G_4S, $(G_4S)2$, the 218 linker, $(G_4S)3$, enzymatically cleavable linker or pH cleavable linker or any similar such linker as would be well known to a person having ordinary skill in this art.

In another embodiment of the present invention, there is provided a method of using the $VEGF_{121}$ fusion conjugate of the present invention to kill cells expressing type 2 VEGF receptors (kinase domain receptor/Flk-1 receptors). The

$VEGF_{121}$ component of the conjugate binds to both VEGF receptor type 1 (Flt-1) and VEGF receptor type 2 (KDR/Flk-1) but is only internalized by cells expressing VEGF receptor type 2. In general, the conjugate is cytotoxic to cells expressing more than 2000 type 2 VEGF receptors per cell.

In yet another embodiment of the present invention, there is provided a method of using the $VEGF_{121}$ fusion conjugate of the present invention to inhibit tumor growth or inhibit metastatic spread and vascularization of metastases in an animal or a human. The method involves the use of a biologically effective amount of the conjugate to exert cytotoxic effect on the tumor vasculature. The method may further comprise treatment with chemotherapeutic agents or radiotherapeutic agents. Representative chemotherapeutic and radiotherapeutic agents are well-known in the art.

The present invention further provides a method of using the $VEGF_{121}$ fusion conjugate of the present invention to inhibit osteoclastogenesis or treat osteoporosis in an animal or a human.

The following examples are given for the purpose of illustrating various embodiments of the invention and are not meant to limit the present invention. The present examples, along with the methods, procedures, treatments, and specific compounds described herein are representative of preferred embodiments. One skilled in the art will appreciate that the present invention is well adapted to carry out the objects and obtain the advantages mentioned, as well as those objects, ends and advantages inherent herein. Changes therein and other uses which are encompassed within the spirit of the invention as defined by the scope of the claims will occur to those skilled in the art.

EXAMPLE 1

Cell Lines And Reagents

Endothelial cell growth supplement from bovine neural tissue was obtained from Sigma. Murine brain endothelioma bEnd.3 cells were provided by Werner Risau (Max Plank Institute, Munich, Germany). Porcine aortic endothelial cells (PAE) transfected with either the human FLT-1 receptor (PAE/FLT-1) or the KDR receptor (PAE/KDR) were provided by Dr. J. Waltenberger. Soluble mouse

Flk-1 was expressed in Sf9 cells as described by Warren *et al.* (1995). The human melanoma A-375 M cell line, human breast cancer SKBR3-HP, and HuT-78 cells were obtained from American Type Culture Collection. Tissue culture reagents were from GIBCO/BRL or Mediatech Cellgro (Herndon, VA).

Rabbit anti-gelonin antisera was obtained from the Veterinary Medicine Core Facility at M.D. Anderson Cancer Center. Anti-flt-1 (sc-316), anti-flk-1 (sc-504), and anti-PARP (sc-8007) antibodies were purchased from Santa Cruz Biotechnology, Inc. (Santa Cruz, CA). BALB/c nude mice were purchased from The Jackson Laboratory and maintained under sterile pathogen-free conditions according to American Association of Laboratory Animal Care standards.

Anti-granzyme B mouse monoclonal antibody, and anti-caspase antibodies were obtained from Santa Cruz Biotechnology (Santa Cruz, CA). Horseradish peroxidase-goat anti-mouse (HRP-GAM) or anti-rabbit conjugate were purchased from Bio-Rad (Hercules, CA). FITC-coupled anti-mouse IgG was obtained from Sigma Chemical Co. (St. Louis, MO). Cytochrome c release apoptosis assay kit was purchased from Oncogene Research Products (Boston, MA). In situ cell death detection kit, AP [terminal deoxynucleotidyl transferase-mediated nick end labeling (TUNEL) assay], and Fast Red were from Roche Molecular Biochemicals (Indianapolis, IN).

The PCR reagents were obtained from Fisher Scientific, and the molecular biology enzymes were purchased from Roche Molecular Biochemicals or New England Biolabs. Bacterial strains, pET bacterial expression plasmids, and recombinant enterokinase were obtained from Novagen. All other chemicals were obtained from Sigma or Fisher Scientific. Metal affinity resin (Talon) was obtained from CLONTECH. Other chromatography resin and materials were purchased from Amersham Pharmacia.

EXAMPLE 2

Construction of $VEGF_{121}$/rGelonin Fusion Toxin

The cDNA encoding human $VEGF_{121}$ and recombinant gelonin were fused together by using the splice overlap extension PCR method with VEGF and gelonin DNA as templates. Primers used were: VEGF Nterm, (5'-

TGGTCCCAGGCTCATATGGCACCCATGGCAGAA-3', SEQ ID NO. 1); VEGF Cterm, (5'-TCTAGACCGGAGCCACCGCCACCCCGCCTCGGCTTGTC-3', SEQ ID NO. 2); Gel Nterm, (5'-GGTGGCGGTGG CTCCGGTCTAGACACCGTGAGC-3', SEQ ID NO. 3); Gel Cterm, (5'-AAG GCTCGTGTCGACCTCGAGTCATTAAGCTTTAGGATCTTTATC- 3', SEQ ID NO. 4). A G4S linker was incorporated between the $VEGF_{121}$ and the rGel sequences. Purified PCR products were digested with the restriction enzymes *Bsp*HI and *Xho*I and ligated into pET-32a. The constructs were transformed into *Escherichia coli* strain AD494 (DE3) pLys S for expression of the fusion protein.

The combination of $VEGF_{121}$ and recombinant gelonin was originally prepared in two different orientations (Figure 1) with both orientations displaying similar cytotoxicity profiles. However, the orientation with $VEGF_{121}$ at the N-terminus results in a higher yield following purification from bacteria, and is used in subsequent experiments.

EXAMPLE 3

$VEGF_{121}$/rGelonin Expression in *E. coli* And Purification

The expression and purification of $VEGF_{121}$/rGel has been previously described (Veenendaal et al., 2002). Bacterial colonies transformed with the plasmid carrying the $VEGF_{121}$/rGel insert were cultured in LB growth medium (Sigma) containing 200 mg/ml ampicillin, 70 mg/ml chloramphenicol, and 15 mg/ml kanamycin at 37°C overnight in a shaker bath at 240 rpm. The cultures then were diluted 1:20 with fresh LB medium with antibiotics and grown to early log phase (A600/0.6) at 37°C. Thereafter, the cultures were diluted 1:1 with fresh LB medium plus antibiotics. Protein synthesis was induced at 23°C by the addition of 0.1 mM isopropyl b-D-thiogalactoside (IPTG) overnight. The cells were collected by centrifugation, resuspended in 10 mM Tris/HCl (pH 8.0), and frozen.

The fusion protein was expressed and purified from bacterial supernatant. *E. coli* cells were lysed with 100 ml 0.1mm glass beads (BioSpec Products, Inc) in a Bead Beater (BioSped Products, Inc) for eight cycles of 3 minutes each. The lysate was ultracentrifuged at 40,000 rpm for 90 minutes at 4°C. The supernatant was carefully collected and adjusted to 40 mM Tris-HCl (pH 8.0), 300

mM NaCl, and incubated at 4°C with metal affinity resin. The resin was washed with 40 mM Tris-HCl (pH8.0), 0.5 M NaCl buffer containing 5 mM Imidazole and eluted with buffer containing 100 mM Imidazole. After pooling fractions containing $VEGF_{121}$/rGel, the sample was dialyzed against 20 mM Tris (pH 8.0), 200 mM NaCl and digested with recombinant Enterokinase at room temperature. Enterokinase was removed by agarose-linked soybean trypsin inhibitor. Other proteins of non-interest were removed by Q Sepharose Fast Flow resin and metal affinity resin as described previously[26]. $VEGF_{121}$/rGel was concentrated and stored in sterile PBS at –20°C.

SDS/PAGE analysis of protein expression after induction with IPTG showed a new protein at 62 kDa, which is the expected molecular weight for the fusion protein plus the 21 kDa purification tag. This material was purified by binding and elution from IMAC resin. Cleavage with recombinant enterokinase removed the tag resulting in a 42-kDa protein under reducing conditions. The construct migrated as a homodimer at 84 kDa under nonreducing conditions. The fusion construct was immunoreactive with antibodies to both VEGF and rGel. One liter of induced bacterial culture initially contained ~2,000 mg of soluble fusion construct. Initial IMAC purification resulted in 750 mg of $VEGF_{121}$/rGel product (yield 37.5%), and digestion with recombinant enterokinase generated 400 mg of target protein (yield 20%). Subsequent purification yielded 230 mg of $VEGF_{121}$/rGel final product (11.5% overall yield).

EXAMPLE 4

Anti-VEGF and Anti-rGel Western Blot Analysis

Protein samples were analyzed by SDS/15% PAGE under reducing conditions. The gel was electrophoretically transferred to nitrocellulose overnight at 4°C in transfer buffer (25 mM Tris/HCl, pH 7.6/190 mM glycine/ 20% HPLC-grade methanol). The membranes were blocked by the addition of 5% BSA in Western blocking buffer [(TBS)/ Tween] and then incubated for 1 h with rabbit anti-gelonin polyclonal antibody (2 mg/ml in TBS/Tween) or mouse anti-VEGF monoclonal antibody 2C3 (2 mg/ml in TBS/Tween). The membrane then was incubated with goat-anti-rabbit IgG horseradish peroxidase (HRP) or goat-anti-mouse IgG-HRP (1: 5,000 dilution in TBS/Tween). Then, the membrane was developed with the Amersham

Pharmacia enhanced chemiluminescence (ECL) detection system and exposed to x-ray film.

EXAMPLE 5

Biological Activity of the rGel Component

The functional activity of rGel and $VEGF_{121}$/rGel were assayed by using a cell-free protein translation inhibition assay kit from Amersham Pharmacia as described by the manufacturer. As determined by the rabbit reticulocyte translation assay, the purified $VEGF_{121}$/rGel and rGel had IC_{50} values of ~47 and 234 pM, respectively, showing that fusion of rGel and $VEGF_{121}$ did not reduce the activity of the toxin component (Figure 2).

EXAMPLE 6

Binding of $VEGF_{121}$/rGel to Soluble Flk-1 Receptor

Binding to Flk-1 was tested on microtiter plates coated with soluble mouse Flk-1. Plates were treated with 2 mg/ml of NeutrAvidin (Pierce) for 6 h. Purified, biotinylated Flk-1 (Warren et al., 1995) was incubated with NeutrAvidin-coated wells for 2 h. $VEGF_{121}$ or $VEGF_{121}$/rGel was added to the wells at various concentrations in the presence of PBS containing 2% (vol/vol) BSA. After 2 h of incubation, plates were washed and incubated with nonblocking mouse monoclonal anti-VEGF antibody, 2C3 (Brekken et al., 1998), or rabbit polyclonal anti-gelonin IgG. For competition studies of $VEGF_{121}$/rGel and $VEGF_{121}$, binding of the $VEGF_{121}$/rGel fusion protein was detected by using a rabbit anti-gelonin antibody. Mouse and rabbit IgG were detected by HRP-labeled goat anti-mouse and anti-rabbit antibodies, respectively (Dako). Peroxidase activity was measured by adding O-phenylenediamine (0.5 mg/ml) and hydrogen peroxide (0.03% vol/vol) in citrate-phosphate buffer (pH 5.5). The reaction was stopped by the addition of 100 ml of 0.18 M of H_2SO_4. The absorbance was read at 490 nM. In competition experiments, a 10-fold molar excess of $VEGF_{121}$ was premixed with $VEGF_{121}$/rGel before addition to the plate.

As shown in Figure 3, $VEGF_{121}$/rGel and native human $VEGF_{121}$ bind equally well to Flk-1 at all concentrations, indicating that the VEGF component of the

fusion protein is fully capable of binding to Flk-1. The specificity of binding of $VEGF_{121}$/rGel to Flk-1 was confirmed by using a 10-fold molar excess of free $VEGF_{121}$ (Figure 4).

EXAMPLE 7

$VEGF_{121}$/rGel and $VEGF_{121}$-Induced Phosphorylation of KDR

Porcine aortic endothelial cells (PAE/KDR) overexpressing the kinase domain receptor (KDR) were incubated overnight in F-12 culture medium and then incubated at 37°C for 5 min with 100 mM Na3 VO4. VEGF or $VEGF_{121}$/rGel then were added and, at various times, cells were lysed by the addition of a lysis buffer (50 mM Hepes, pH 7.4/150 mM NaCl/1 mM EGTA/10 mM sodium pyrophosphate/1.5 mM MgCl2/100 mM NaF/10% (vol/vol) glycerol/1% Triton X-100). Cell lysates were centrifuged (16,000 x *g*), the supernatants were removed, and their protein concentrations were determined. Lysate supernatants were incubated with 9 mg anti-phosphotyrosine monoclonal antibody (Santa Cruz Biotechnology) for 2 h at 4°C and then precipitated by the addition of Protein A Sepharose beads for 2 h at 4°C. Beads were washed and mixed with SDS sample buffer, heated for 5 min at 100°C, centrifuged, analyzed by SDS/10% PAGE, and then transferred to nitrocellulose filters. The membranes were blocked with 5% nonfat dry milk and incubated with rabbit polyclonal anti-KDR antibody (1:250; Santa Cruz Biotechnology) for 1 h at room temperature. The membranes then were washed, incubated with a peroxidase-linked goat anti-rabbit antibody (1:2,000) for 1 h at room temperature, and then enhanced chemiluminescence reagent (Amersham Pharmacia) was used to visualize the immunoreactive bands.

Results from these experiments showed that addition of $VEGF_{121}$/rGel or $VEGF_{121}$ increased phosphotyrosine content. There were two phases of phosphorylation; an early phase (1–10 min) and a later phase (4–8 h). The time course of induction of KDR phosphorylation was the same for $VEGF_{121}$/rGel and $VEGF_{121}$. Phosphorylation of FLT-1 in PAE/FLT-1 cells treated with either $VEGF_{121}$/rGel or $VEGF_{121}$ was not observed, as expected from the weaker signaling of FLT-1 compared with KDR observed by others.

Although $VEGF_{121}$/rGel induces phosphorylation of KDR receptor, no growth-stimulatory effects of the fusion toxin on VEGF receptor-expressing cells were observed. These findings are in keeping with studies of other fusion toxins such as IL-2/DT that initially stimulate target cells in a manner similar to that of IL-2 itself, but ultimately kill the target cells through the actions of the internalized toxin.

EXAMPLE 8

Cytotoxicity of $VEGF_{121}$/rGel to Endothelial Cells *in vitro*

To determine cytotoxicity on adult bovine aortic arch-derived endothelial cells (ABAE), log-phase adult bovine aortic arch-derived endothelial cells in DMEM [10% (vol/vol) FBS] were diluted to 4,000 cells per 200 ml. Aliquots (200 ml) were added to 96-well flat-bottomed tissue culture plates and incubated at 37°C for 1–72 h in 5% CO_2. Purified $VEGF_{121}$/rGel or rGel were diluted in culture medium to various concentrations, added to the plate, and the cultures were incubated for 72 h. Remaining adherent cells were stained by the addition of 100 ml of crystal violet [0.5% in 20% (vol/vol) methanol]. Dye-stained cells were solubilized by the addition of 100 ml of Sorenson's buffer [0.1M sodium citrate, pH 4.2 in 50% (vol/vol) ethanol]. The absorbance was measured at 595 nM.

To determine cytotoxicity on mouse brain-derived endothelial cells bEnd.3, the cells were seeded at a density of 50,000/well in 24-well plates. Twenty-four hours later, $VEGF_{121}$/rGel or rGel alone were added at various concentrations. After 5 days of treatment at 37°C, remaining attached cells were trypsinized and counted. The results are presented as total cell number per well. Two identical experiments were performed in duplicate. Standard error in all experiments was less than 5% of the mean.

To determine cytotoxicity on PAE/KDR and PAE/FLT-1 cells, log-phase PAE/KDR cells and PAE/FLT-1 cells in F-12 medium [10% (vol/vol) FBS] were diluted to 3,000 cells per 200 ml. Aliquots (200 ml) were added to 96-well flat-bottomed tissue culture plates and incubated at 37°C for 24 h in 5% CO_2. Purified $VEGF_{121}$/rGel or rGel were diluted in culture medium, added to the plate, and incubated for 72 h. Adherent cells were quantified by using the crystal violet staining method described above.

$VEGF_{121}$/rGel was specifically toxic to KDR/Flk-1 expressing endothelial cells *in vitro* (Fig. 5 and Table 1). The IC_{50} values for $VEGF_{121}$/rGel on log-phase PAE/KDR, ABAE, and bEnd.3 cells, which express 1–3 x 10^5 KDR/Flk-1 receptors per cell, was 0.06 to 1 nM. Cells expressing FLT-1 and having low endogenous expression of KDR (PAE/FLT-1, HUVEC) were several hundred-fold more resistant to $VEGF_{121}$/rGel than were the KDR/Flk-1 expressing cells. Thus, FLT-1 appears not to mediate cytotoxicity of $VEGF_{121}$/rGel.

The ratio of IC_{50} values of rGel to $VEGF_{121}$/rGel was calculated for each cell type. This ratio (the targeting index) represents the ability of the VEGF component of the fusion construct to mediate the delivery of the toxin to the endothelial cell surface and into the intracellular ribosomal compartment. As summarized in Table 1, bEnd.3 and adult bovine aortic arch-derived endothelial cells were, respectively, 100-fold and 9-fold more sensitive to the fusion construct than they were to free rGel.

TABLE 1

Number of VEGF Receptors Per Cell And Sensitivity To $VEGF_{121}$/rGel

Cell Type	Number of FLT-1 sites per cell	Number of KDR sites per cell	IC_{50} for $VEGF_{121}$/rGel (nM)	IC_{50} for rGel (nM)	Targeting index *
PAE/KDR (log phase)	0	$2\text{-}3x10^5$	0.5	300	600
PAE/KDR (confluent)	0	$2\text{-}3x10^5$	30	5000	167
bEnd3 (log phase)	Not done	$2x10^5$	1	100	100
ABAE (log phase)	0	$0.4x10^5$	0.059	0.524	8.9
HUVEC (hypoxia)	Not done	$0.023x10^5$	700	>1000	~1
HUVEC (normoxia)	Not done	$0.017x10^5$	800	>1000	~1
PAE/FLT-1 (log phase)	$0.5x10^5$	Not done	300	300	1
PAE/FLT-1 (confluent)	$0.5x10^5$	Not done	>5000	10000	<2
A-375 (log phase)	Not done	Not done	330	109	0.3
PC-3 (log phase)	Not done	Not done	225	100	0.4

* Targeting index is defined as the ratio of IC_{50} of rGel to $VEGF_{121}$/rGel.

EXAMPLE 9

Selective Cytotoxicity of $VEGF_{121}$/rGel for Dividing PAE/KDR Cells

$VEGF_{121}$/rGel was 60-fold more toxic to PAE/KDR cells in log-phase growth than it was to PAE/KDR cells that had been grown to confluence and rested (Table 1). This effect was not caused by differences in KDR expression, because the cells expressed the same number of KDR receptors per cell in both phases of growth. The log-phase PAE/KDR cells also were more sensitive to rGel itself than were the confluent cells, suggesting that the quiescence of confluent cells impacts their sensitivity to both targeted and nontargeted rGel. It is possible that the rate or route of entry of both $VEGF_{121}$/rGel and rGel is different for dividing and nondividing cells.

EXAMPLE 10

$VEGF_{121}$/rGel binds to both KDR and FLT-1

$VEGF_{121}$ has been shown to bind to the FLT-1 receptor with greater affinity than to KDR. Because cytotoxicity of $VEGF_{121}$/rGel to KDR-expressing cells was found to be nearly 600-fold greating than for FLT-1 expressing cells, the relative binding of $VEGF_{121}$/rGel to PAE cells expressing each of the receptors was investigated.

ELISA analysis was performed to confirm the expression of both receptors on the cell surface using receptor-specific antibodies (data not shown). Expression of VEGFR-1 (FLT-1) and VEGFR-2 (KDR) was confirmed by western blot (Figure 6A). Whole cell lysates of PAE/KDR and PAE/FLT-1 cells were obtained by lysing cells in Cell Lysis buffer (50 mM Tris, pH 8.0, 0.1 mM EDTA, 1 mM DTT, 12.5 mM $MgCl_2$, 0.1 M KCl, 20% glycerol) supplemented with protease inhibitors (0.5% leupeptin, 0.5% aprotinin and 0.1% PMSF). Protein samples were separated by SDS-PAGE under reducing conditions and electrophoretically transferred to a PVDF memberane overnight at 4^BC in transfer buffer (25 mM Tris-HCl, pH 7.6, 190 mM glycine, 20% HPLC-grade methanol). The samples were analyzed for KDR with rabbit anti-flk-1 polyclonal antibody and FLT-1 using an anti-flt-1 polyclonal antibody. The membranes were then incubated with goat-anti-rabbit IgG horseradish peroxidase (HRP), developed using the Amersham ECL detection system and exposed to X-ray film.

In order to confirm that $VEGF_{121}$/rGel bound to human VEGFR-1 and VEGFR-2 and that the presence of recombinant gelonin did not interfere with the binding properties of $VEGF_{121}$, the binding of radiolabeled $VEGF_{121}$/rGel to both KDR and FLT-1 receptors expressed on the surface of PAE cells was investigated. One hundred μg of $VEGF_{121}$/rGel was radiolabeled with 1mCi of NaI^{125} using Chloramine T^{27} for a specific activity of 602 Ci/mMol. Cells were grown overnight in 24-well plates. Non-specific binding sites were blocked for 30 minutes with PBS/0.2% gelatin followed by incubation for 4 hours with ^{125}I-$VEGF_{121}$/rGel in PBS/0.2% gelatin solution. For competition experiments, cold $VEGF_{121}$/rGel or gelonin were pre-mixed with ^{125}I-$VEGF_{121}$/rGel. Cells were washed four times with PBS/0.2% gelatin solution, detached and bound cpm was measured.

Figure 6B shows that the binding of ^{125}I-$VEGF_{121}$/rGel to both cells was nearly identical. Binding of $VEGF_{121}$/rGel to both PAE/KDR and PAE/FLT-1 cells was competed by unlabeled $VEGF_{121}$/rGel but not by unlabeled gelonin, indicating that binding of $VEGF_{121}$/rGel was mediated by $VEGF_{121}$.

EXAMPLE 11

Internalization of $VEGF_{121}$/rGel into PAE/KDR cells

The internalization of $VEGF_{121}$/rGel into PAE/KDR and PAE/FLT-1 cells was investigated using immunofluorescence staining. PAE/KDR and PAE/FLT-1 cells were incubated with 4 μg/ml $VEGF_{121}$/rGel at various time points. After stripping the cell surface, cells were fixed with 3.7% formaldehyde and permeabilized with 0.2% Triton X-100. Non-specific binding sites were blocked with 5% BSA in PBS. Cells were then incubated with a rabbit anti-gelonin polyclonal antibody (1:200) followed by a TRITC-conjugated anti-rabbit secondary antibody (1:80). Nuclei were stained with propidium iodide (1μg/ml) in PBS. The slides were fixed with DABCO media, mounted and visualized under fluorescence (Nikon Eclipse TS1000) and confocal (Zeiss LSM 510) microscopes.

$VEGF_{121}$/rGel was detected in PAE/KDR cells within 1 hour of treatment with the immunofluoresence signal progressively increasing to 24 hours (Figure 7). As expected, cell density also decreased over the 24 hour time period. No $VEGF_{121}$/rGel was detected in PAE/FLT-1 cells up to 24 hours after treatment with

the fusion toxin. Treatment of cells with the same concentration of rGelonin showed no internalization, confirming that entry of $VEGF_{121}$/rGel into PAE cells was specifically via the KDR receptor.

EXAMPLE 12

Cytotoxic Effects of $VEGF_{121}$/rGel As A Function of Exposure Time on Endothelial Cells

The IC_{50} of $VEGF_{121}$/rGel incubated for 72 hours on log-phase PAE/KDR cells has been shown to be about 1 nM. However, $VEGF_{121}$/rGel internalizes into these cells within one hour of incubation. To study the cytototoxic effect of $VEGF_{121}$/rGel as a function of exposure time of this agent on endothelial cells, cells were incubated with $VEGF_{121}$/rGel from 1-72 hours and its cytotoxicity on PAE/KDR cells was assessed at the end of the 72-hour period.

While $VEGF_{121}$/rGel retained cytotoxicity even after a one hour incubation, appreciable cytotoxicity was observed after 24 hours and maximal cytotoxic effect of $VEGF_{121}$/rGel on PAE/KDR cells was observed after 48 hours (Figure 8). The cytotoxic effect of $VEGF_{121}$/rGel on PAE/FLT-1 cells was also affected as a function of exposure duration (data not shown).

EXAMPLE 13

Cytotoxic Mechanism of $VEGF_{121}$/rGel

In order to investigate the mechanism of cytotoxicity of $VEGF_{121}$/rGel to PAE/KDR cells, a TUNEL assay was performed for 24, 48 and 72 hours. Log phase PAE/KDR and PAE/FLT-1 cells were diluted to 2000 cells/100 µl. Aliquots (100 µl) were added in 16-well chamber slides (Nalge Nunc International) and incubated overnight at 37°C with 5% CO_2. Purified $VEGF_{121}$/rGel was diluted in culture media and added at 72, 48 and 24 hour time points at a final concentration of 1 nM (twice the IC_{50}). The cells were then processed and analyzed for TUNEL as described by the manufacturer of the reagent. Positive control cells were incubated with 1 mg/ml DNAse for 10 minutes at 37°C.

No TUNEL staining was observed with PAE/KDR cells exposed to $VEGF_{121}$/rGel up to 72 hours (Figure 9). In contrast nuclei of positive control cells

showed intense staining, indicating that the mechanism of cytotoxicity of $VEGF_{121}$/rGel is not apoptotic.

Effects of $VEGF_{121}$/rGel on PARP-mediated apoptosis were investigated by pre-incubating PAE/KDR cells with 100 mM Na_2VO_4 for 5 minutes at 37°C followed by stimulation with $VEGF_{121}$/rGel or $VEGF_{121}$ for 5 minutes, 30 minutes, 4 h, 24 h and 48 h. Cells were washed and lysed. Cell lysate was analyzed by Western using an anti-PARP antibody. Western blot analysis of these cells showed that $VEGF_{121}$/rGel did not activate PARP-mediated apoptosis (Figure 10).

EXAMPLE 14

Inhibition of Tumor Growth *in vivo* by $VEGF_{121}$/rGel

Human melanoma xenograft model was established as follows. Female nu/nu mice were divided into groups of five mice each. Log-phase A-375M human melanoma cells were injected s.c. ($5x10^6$ cells per mouse) into the right flank. After the tumors had become established (~50 mm^3), the mice were injected with $VEGF_{121}$/rGel through a tail vein five times over an 11 day period. The total dose of $VEGF_{121}$/rGel was 17 or 25 mg/kg. Other mice received rGel alone at a dose totaling 10 mg/kg. Mice were killed by cervical dislocation after the 40th day of tumor measurement.

Human prostate cancer xenograft model was established as follows. Male nude mice weighing ~20 g were divided into groups of five mice each. Log-phase PC-3 human prostate tumor cells were injected s.c. (5×10^6 cells per mouse) in the right flank. The mice were injected with $VEGF_{121}$/rGel through a tail vein every 2–3 days for 11 days. The total dose of $VEGF_{121}$/rGel was 20 mg/kg. Other mice received rGel alone at a dose totaling 10 mg/kg. Tumor volume was calculated according to the formula: volume = L x W x H, where L = length, W = width, H = height.

As shown in Figure 11, saline-treated human melanoma A-375M tumors showed an increase in tumor volume 24-fold (from 50 mm^3 to 1200 mm^3) over the 30-day observation period. Treatment of the mice with $VEGF_{121}$/rGel strongly retarded tumor growth. At high doses of $VEGF_{121}$/rGel totaling 25 mg/kg, tumor growth was completely prevented, but all mice died from drug toxicity on day 19. At lower doses totaling 17 mg/kg, all mice survived. Tumor growth was completely

prevented throughout the 14-day course of treatment, but thereafter, tumor regrowth slowly recurred. Compared with controls, mice treated with $VEGF_{121}$/rGel at doses totaling 17 mg/kg showed a 6-fold decrease in tumor volume (1,200 mm^3 vs. 200 mm^3).

Human prostatic carcinoma (PC-3) tumors increased 12-fold in volume during the 26-day observation period (Figure 12). Treatment of the mice with five doses of $VEGF_{121}$/rGel totaling 20 mg/kg virtually abolished tumor growth, even after cessation of treatment. Tumor volume in the treated group only increased from 100 to 200 mm^3 over the course of the experiment. Compared with controls, treatment with $VEGF_{121}$/rGel resulted in a 7-fold decrease in tumor volume (1,400 mm^3 vs. 200 mm^3).

EXAMPLE 15

Localization of $VEGF_{121}$/rGel to Vascular Endothelium in Prostate Tumor Xenografts

Mice (three mice per group) bearing PC-3 human prostate tumors were injected intravenously with 50 ug of the fusion protein gelonin (2.5 mg/kg) or free gelonin (1 mg/kg). The mean tumor volume per group was 260 mm^3. Thirty minutes later, mice were killed, exsanguinated, and all major tissues were snap frozen. Frozen sections were cut and double stained with pan-endothelial marker MECA-32 (5 mg/ml) followed by detection of the localized fusion protein using rabbit anti-gelonin antibody (10 mg/ml). MECA-32 rat IgG was visualized with goat anti-rat IgG conjugated to FITC (red fluorescence). Anti-gelonin antibody was detected with goat anti-rabbit IgG conjugated to Cy-3 (green fluorescence). Colocalization of both markers was indicated by a yellow color. Anti-gelonin antibody had no reactivity with tissue sections from mice injected with saline or $VEGF_{121}$. To determine the percentage of vessels with localized fusion protein, the number of vessels stained with MECA-32 (red), gelonin (green), or both (yellow) were counted at a magnification of x200 in at least 10 fields per section. Two slides from each mouse were analyzed, and the average percentage of positive vessels was calculated.

As shown in Figure 13, $VEGF_{121}$/rGel was detected primarily on vascular endothelium of PC-3 tumors (Fig. 13). On average, 62% of vessels positive for MECA 32 were also positive for $VEGF_{121}$/rGel, as detected by using anti-gelonin antibody. In tumor regions of increased vascularity (''hot spots''), approximately

90% of tumor vessels had bound $VEGF_{121}$/rGel. Vessels in normal organs were unstained, with the exception of the kidney, where weak and diffuse staining was detected in the glomeruli. Free gelonin did not localize to tumor or normal vessels in any of the mice. These results indicate that $VEGF_{121}$/rGel localized specifically to tumor vessels after i.v. injection.

EXAMPLE 16

Destruction and Thrombosis of Tumor Vessels by $VEGF_{121}$/rGel

Mice bearing s.c. PC-3 tumors were given one i.v. dose of $VEGF_{121}$/rGel (2.5 mg/kg) or saline. The mice were killed 48 h later, and the tumors and various organs were removed. Paraffin sections were prepared and stained with hematoxylin and eosin. The tumors from $VEGF_{121}$/rGel recipients (Fig. 14) displayed damaged vascular endothelium, thrombosis of vessels, and extravasation of RBC components into the tumor interstitium. Normal tissues had un-damaged vasculature. Treatment of mice with saline had no effect on tumor or normal tissues. As assessed by image analysis, necrotic areas of the tumor increased from ~4% in saline-treated mice to ~12% after treatment with the fusion construct.

EXAMPLE 17

Cytotoxicity of $VEGF_{121}$/rGel On MDA-MB-231 Breast Tumor Cells

As assessed by Western blot, MDA-MB-231 breast cancer cells do not appear to express VEGFR-1 or VEGFR-2, the receptors which bind $VEGF_{121}$ (Figure 15A). Cytotoxicity of $VEGF_{121}$/rGel and rGel against log phase MDA-MB-231 cells was determined as follows. Cells were grown in 96-well flat-bottom tissue culture plates. Purified $VEGF_{121}$/rGel and rGel were diluted in culture media and added to the wells in 5-fold serial dilutions. Cells were incubated for 72 hours. The remaining adherent cells were stained with crystal violet (0.5% in 20% methanol) and solubilized with Sorenson's buffer (0.1 M sodium citrate, pH 4.2 in 50% ethanol). Absorbance was measured at 630 nm. As shown in Figure 15B, the cytotoxicity of $VEGF_{121}$/rGel on MDA-MB-231cells showed an IC_{50} slightly higher than that observed for recombinant gelonin, indicating that $VEGF_{121}$/rGel does not have a specific target on MBA-MB-231 cells.

EXAMPLE 18

Localization of $VEGF_{121}$/rGel to Vascular Endothelium in Breast Tumor Xenografts

SCID mice (3 mice per group) bearing orthotopic MDA-MB-231 tumors were intravenously injected with 50 ug of the fusion protein or equivalent amount of free gelonin. The mean tumor volume per group was 260 mm^3. Four hours later the mice were sacrificed and exsanguinated. All major organs and tumor were harvested and snap-frozen for preparation of cryosections.

Frozen sections were double stained with a pan-endothelial marker MECA 32 (5 ug/ml) followed by detection of the localized fusion protein using rabbit anti-gelonin antibody (10 ug/ml). MECA 32 rat IgG (provided by Dr. E. Butcher of Stanford University, CA) was visualized by goat anti-rat IgG conjugated to FITC (green fluorescence). Rabbit anti-gelonin antibody was detected by goat anti-rabbit IgG conjugated to Cy-3 (red fluorescence).

Co-localization of both markers was indicated by yellow color. Anti-gelonin antibody had no reactivity with tissues sections derived from mice injected with saline or with $VEGF_{121}$. To determine % of vessels with localized fusion protein, MECA 32 positive, gelonin-positive and vessels with combined color were counted at magnification of x 200 in at least 10 fields per section. Two slides from each mouse were analyzed and percent of positive vessels was averaged.

As shown in Figure 16, $VEGF_{121}$/rGel was primarily detected on endothelium of tumor. In average, sixty percent of vessels positive for MECA 32 were also positive for gelonin in the group of $VEGF_{121}$/rGel –injected mice. In the tumor regions of increased vascularity (hot spots), up to 90% of tumor vessels were labeled by anti-gelonin IgG. Vessels with bound $VEGF_{121}$/rGel were homogeneously distributed within the tumor vasculature. Vessels in normal organs were unstained with the exception of the kidney where weak and diffuse staining was detected in the glomeruli. Free gelonin did not localize to tumor or normal vessels in any of the mice, indicating that only targeted gelonin was able to bind to the tumor endothelium. These results indicate that $VEGF_{121}$/rGel specifically localizes to tumor vessels that demonstrate high density and favorable distribution of $VEGF_{121}$/rGel–binding sites.

EXAMPLE 19

Metastatic Model of MDA-MB-231 Tumors

The following examples utilize a breast cancer pulmonary metastatic model to establish $VEGF_{121}$/rGel fusion toxin can inhibit metastatic spread and vascularization of metastases.

Human breast carcinoma MDA-MB-231 cells consistently lodge in lungs following intravenous injection into the tail vein of athymic or SCID mice. Micrometastases are first detected 3 to 7 days after injection of $5x10^5$ cells and macroscopic colonies develop in 100% of the injected mice within 4 to 7 weeks. Mortality occurs in all mice within 10-15 weeks. This model of experimental breast cancer metastasis examines the ability of tumor cells to survive in the blood circulation, extravasate through the pulmonary vasculature and establish growing colonies in the lung parenchyma.

Female SCID mice, aged 4-5 weeks, were injected in a tail vein with 0.1 ml of MDA-MB-231 cell suspension ($5x10^5$ cells). The mice were randomly separated into two groups (6 mice per group) and were treated with either $VEGF_{121}$/rGel or gelonin alone (100 μg intraperitoneally, 6 times total with an interval of 3 days) starting the 8^{th} day after the injection of cells. Treatment with $VEGF_{121}$/rGel for 2 weeks allow the mice to receive the maximal tolerated accumulative dose of the drug (600 μg per mouse). Prior studies established that $VEGF_{121}$/rGel given at such dose did not cause histopathological changes in normal organs. The accumulative dose of 640-800 μg of total $VEGF_{121}$/rGel fusion protein, given i.p. over period of 4 weeks, did not induce significant toxicity as judged by morphological evaluation of normal organs. Transient loss of weight (~10%) was observed 24 hours after most of the treatments with complete weight recovery thereafter.

Metastatic colonies were allowed to expand for three weeks after treatment with $VEGF_{121}$/rGel in order to evaluate long-term effect of $VEGF_{121}$/rGel on the size of the colonies, proliferation index of tumor cells and their ability to induce new blood vessel formation. Three weeks after termination of the treatment, the animals were sacrificed and their lungs were removed. One lobe was fixed in Bouin's fixative and the other lobe was snap-frozen. After fixation in Bouin's fixative, the

tumor colonies on the lung surface appear white, whereas the normal lung tissue appears brown. The number of tumor colonies on the surface of each lung was counted and the weight of each lung was measured. The values obtained from individual mice in the $VEGF_{121}$/rGel and rGel groups were averaged per group.

EXAMPLE 20

Effects of $VEGF_{121}$/rGel on the Number, Size And Vascular Density of MDA-MB-231 Pulmonary Metastatic Foci

Frozen samples of lung tissue was cut to produce sections of 6 μm. Blood vessels were visualized by MECA 32 antibody and metastatic lesions were identified by morphology and by 6w/32 antibody directed against human HLA antigens. Hybridoma producing the mouse monoclonal 6w/32 antibody was purchased from ATCC. The 6w/32 antibody was purified from hybridoma supernatant using Protein A resin.

Each section was double stained by MECA 32 and 6w/32 antibodies to ensure that the analyzed blood vessels are located within a metastatic lesion. Slides were first viewed at low magnification (x2 objective) to determine total number of foci per a cross-section. Six slides derived from individual mice in each group were analyzed and the number was averaged. Images of each colony were taken using digital camera (CoolSnap) at magnifications of x40 and x100 and analyzed using Metaview software that allows measurements of smallest and largest diameter, perimeter (μm) and area (mm^2).

The vascular endothelial structures identified within a lesion were counted and number of vessels per each lesion was determined and normalized per mm^2. The mean number of vessels per mm^2 was calculated per each slide and averaged per $VEGF_{121}$/rGel and rGel groups (6 slides per group). The results are expressed ± SEM. The same method applied to determine the mean number of vessels in non-malignant tissues.

Treatment with $VEGF_{121}$/rGel but not with free gelonin significantly reduced both the number of colonies per lung and the size of the metastatic foci present in lung by 42-58% as shown in Figure 17 and Table 2.

The overall mean vascular density of lung colonies was reduced by 51% compared to the rGel treated controls (Table 3 and Figure 18). The observed effect, however, was non-uniformly distributed among different tumor colony sizes. The greatest impact on vascularization was observed on mid-size and extremely small tumors (62 and 69% inhibition respectively) while large tumors demonstrated the lease effect (10% inhibition). The majority of lesions in the $VEGF_{121}$/rGel-treated mice (~70%) were avascular whereas only 40% of lesions from the control group did not have vessels within the metastatic lung foci.

TABLE 2

Effect of $VEGF_{121}$/rGel on Number And Size of Pulmonary Metastases of MDA-MB- 231 Human Breast Carcinoma Cells

Parameter	Treatment [a]		% inhibition *vs.* rGelonin treatment	P value [b]
	rGelonin	$VEGF_{121}$/rGel		
No. surface colonies per lung (range) [c]	53.3 ± 22 (33-80)	22.4 ± 9.2 (11-41)	58.0%	0.03
No. intraparenchymal colonies per cross-section (range) [d]	22 ± 7.5 (18-28)	12.8 ± 5.5 (5-18)	42.0%	0.02
Mean area of colonies (μm) [e]	415 ± 10	201 ± 37	51.9%	0.01
Mean % of colonies-occupied area per lung section [f]	57.3 ± 19	25.6 ± 10.5	55.4%	0.01

[a] Mice with MDA-MB-231 pulmonary micrometastases were treated i.p. with $VEGF_{121}$/rGel or free gelonin as described.

[b] P value was calculated using t-Student test.

[c] Lungs were fixed with Bouin's fixative for 24 hours. Number of surface white colonies was determined for each sample and averaged among 6 mice from $VEGF_{121}$/rGel or rGel control group. Mean number per group ± SEM is shown. Numbers in parentheses represent range of colonies in each group.

[d] Frozen sections were prepared from metastatic lungs. Sections were stained with 6w/32 antibody recognizing human tumor cells. Number of intraparenchymal colonies identified by brown color was determined for each cross-section and averaged among 6 samples of individual mice from $VEGF_{121}$/rGel or rGel control group. Mean number per group ± SEM is shown. Numbers in parentheses represent range of colonies in each group.

[e] Area of foci identified by 6w/32 antibody was measured by using Metaview software. Total number of evaluated colonies was 101 and 79 for rGel and $VEGF_{121}$/rGel group, respectively. Six individual slides per each group were analyzed. The mean area of colony in each group ± SEM is shown.

[f] The sum of all regions occupied by tumor cells and the total area of each lung cross-section was determined and % of metastatic regions from total was calculated. The values obtained from each slide were averaged among 6 samples from $VEGF_{121}$/rGel or rGel control group. The mean % area occupied by metastases from total area per group ± SEM is shown.

TABLE 3

Effect of $VEGF_{121}$/rGel On Vascularity of Pulmonary Metastases of MDA-MB- 231 Human Breast Carcinoma Cells

Size of colonies [a]	Largest diameter range (μm)	No. vascularized colonies from total analyzed (%) [b]		% Inhibition vs. radiation treatment
		rGel	$VEGF_{121}$/rGel	
Extremely small	<50	7/24 (29%)	3/32 (9.3%)	69
Small	50-200	19/48 (39.5%)	6/24 (25%)	37
Mid-size	200-500	25/30 (83.3%)	8/25 (32%)	62
Large	500-1000	17/17 (100%)	10/11 (90.0%)	10
Extremely large	>1000	8/8 (100%)	N/A	N/A
No. vascular foci/ total analyzed (%) [c]		76/127 (59.8%)	27/92 (29.3%)	51

[a] Colonies identified on each slide of a metastatic lung were subdivided into 5 groups according to their largest diameter. [b] Frozen lung sections from $VEGF_{121}$/rGel or rGel treated mice were stained with MECA 32 antibody. A colony was defined as vascularized if at least one blood vessel branched out from the periphery and reached a center of the lesion. Six slides per each group derived from individual mice were analyzed and data were combined. [c] Total number of the analyzed colonies was 127 and 92 for rGel and $VEGF_{121}$/rGel treated groups, respectively. Seventy percent of foci in the $VEGF_{121}$/rGel-treated group were avascular whereas only 40% of lesions from the control group did not have vessels within the metastatic foci.

EXAMPLE 21

Effect of $VEGF_{121}$/rGel On The Number of Cycling Cells In The MDA-MB-231 Pulmonary Metastatic Foci

Frozen sections of normal mouse organs and metastatic lungs were fixed with acetone for 5 min and rehydrated with PBST for 10 min. All dilutions of antibodies were prepared in PBST containing 0.2% BSA. Primary antibodies were detected by appropriate anti-mouse, anti-rat or anti-rabbit HRP conjugates (Daco, Carpinteria, CA). HRP activity was detected by developing with DAB substrate (Research Genetics).

To determine the number of cycling cells, tissue sections were stained with the ki-67 antibody (Abcam, Inc., Cambridge, UK) followed by anti-mouse IgG HRP conjugate. Sections were analyzed at magnification of x100. Number of cells positive for ki-67 was normalized per mm^2. The mean number ± SD per $VEGF_{121}$/rGel or control group is presented. The average numbers derived from analysis of each slide were combined per either $VEGF_{121}$/rGel or rGel group and analyzed for statistical differences.

The number of cycling tumor cells in lesions from the $VEGF_{121}$/rGel group was reduced by ~60% as compared to controls (Figure 19). The overall mean vascular density of lung colonies was reduced by 51% (Table 3 and Figure 18). These findings suggest that vascularity of metastases directly affects tumor cell proliferation.

EXAMPLE 22

Effect of $VEGF_{121}$/rGel on flk-1 Expression in Tumor Vessel Endotheluim of The MDA-MB-231 Pulmonary Metastatic Foci

The expression of VEGF receptor-2 on the vasculature of breast tumors metastatic to lung was assessed using the RAF-1 antibody. Frozen sections of lungs from mice treated with $VEGF_{121}$/rGel or free gelonin were stained with monoclonal rat anti-mouse VEGFR-2 antibody RAFL-1 (10 μg/ml). RAFL-1 antibody was detected by goat anti-rat IgG-HRP. The expression of KDR on the remaining few vessels present in lung metastatic foci demonstrated a significant decline compared to that of lung foci present in control tumors (Figure 20). This suggests

that the $VEGF_{121}$/rGel agent is able to significantly down-regulate the receptor or prevent the outgrowth of highly receptor-positive endothelial cells.

EXAMPLE 23

Summary of the Biological Properties of $VEGF_{121}$/rGel

$VEGF_{121}$/rGel was found to be selectively toxic to dividing endothelial cells overexpressing the KDR/Flk-1 receptor. Nondividing (confluent) endothelial cells were almost 60-fold more resistant than were dividing cells to the fusion construct and also were more resistant to free gelonin (Table 1). These findings accord with those of previous studies that showed conjugates of vascular endothelial growth factor and diphtheria toxin were highly toxic to log-phase cells but were not toxic to confluent endothelial cells. The greater sensitivity of dividing endothelial cells to VEGF-toxin constructs may be because of differences in intracellular routing or catabolism of the construct as observed with other targeted therapeutic agents.

Cytotoxicity studies demonstrated that expression of the KDR/Flk-1 receptor is needed for $VEGF_{121}$/rGel to be cytotoxic. Cells overexpressing KDR/Flk-1 ($>1 \times 10^5$ sites per cell) were highly sensitive to the $VEGF_{121}$/rGel fusion construct, whereas cells expressing fewer than 0.4×10^5 sites per cell were no more sensitive to the fusion toxin than they were to free gelonin. Again, the requirement to surpass a threshold level of KDR/Flk-1 for cytotoxicity may contribute to the safety of $VEGF_{121}$/rGel. In normal organs, including the kidney glomerulus and pulmonary vascular endothelium, the level of KDR/Flk-1 may be below that needed to cause toxicity. The number of receptors for vascular endothelial growth factor on endothelial cells in the vasculature of normal organs has been reported to be significantly lower than on tumor vasculature. Indeed, one could not detect binding of $VEGF_{121}$/rGel to normal vascular endothelium in organs other than the kidney, where weak binding was observed. Furthermore, no damage to vascular endothelium was observed in normal organs, including the kidney.

Other gelonin-based-targeted therapeutics also have been observed to become toxic to cells only when a certain threshold level of binding is surpassed. In a recent study of immunotoxins directed against the c-erb-2/HER2/neu oncogene product, immunotoxins were not cytotoxic to tumor cells expressing less than about 1

x 10^6 HER2/neu sites per cell. The lack of sensitivity of cells having low levels of receptors is presumably because the cells internalize too little of the toxin or traffic it to compartments that do not permit translocation of the toxin to the ribosomal compartment.

Although VEGF/rGel fusion can bind to both the KDR and FLT-1 receptors, only cells expressing KDR were able to internalize the construct thereby delivering the toxin component to the cytoplasmic compartment. It has been suggested that it is the interaction of vascular endothelial growth factor with the KDR receptor but not the FLT-1 receptor that is responsible for the growth proliferative signal on endothelial cells. Other studies suggest that the KDR receptor is primarily responsible for mediating the vascular permeability effects of VEGF-A. Although FLT-1 receptor may modulate signaling of the KDR receptor and impact monocyte response to vascular endothelial growth factor, its role in neovascularization has not been well-defined.

The presence of FLT-1, even at high levels, does not seem to mediate cellular toxicity of the $VEGF_{121}$/rGel fusion toxin. Although VEGF binds to the FLT-1 receptor, the current study has been unable to demonstrate receptor phosphorylation as a result of ligand binding. It has been suggested that receptor phosphorylation may be required for KDR signaling and internalization. If so, the receptor–fusion–toxin complex may not internalize efficiently after binding to FLT-1 for the fusion protein to be routed to an intracellular compartment from which the toxin can escape to the cytosol. The relative contributions of the FLT-1 and KDR receptors to the biological effects of vascular endothelial growth factor examined by using a monoclonal antibody that blocks the interaction of vascular endothelial growth factor with KDR/Flk-1 but not FLT-1 demonstrate that KDR/Flk-1 is the major receptor determining the vascular permeability-inducing and angiogenic effects of vascular endothelial growth factor in tumors.

Another important observation was that the cytotoxic effects of the $VEGF_{121}$/rGel construct on vascular endothelial cells did not involve an apoptotic mechanism. This is in sharp contrast to studies of other toxins such as ricin A chain (RTA) and pseudomonas exotoxin (PE) which demonstrate generation of apoptotic effects that are mediated, at least in part, by caspase activation. It has been suggested

that PE toxins may generate cytotoxic effects through both caspase-dependant and protein synthesis inhibitory mechanisms. Despite the sequence homology of ricin A chain and rGel and the known similarities in their mechanism of action, it appears that these two toxins differ in their pro-apoptotic effects. One possible explanation for the observed differences in apoptotic effects between ricin A chain and the rGel toxin could be in the cell types examined. The cells targeted in the current study of rGel are non-transformed endothelial cells while those in the ricin A chain study were tumor cells.

The exposure duration studies for the $VEGF_{121}$/rGel fusion toxin demonstrate that as little as 1 hr exposure to target cells is required to develop a cytotoxic effect 72 hrs later. However, continual exposure for up to 48 hrs was shown to improve the cytotoxic effect by almost 10 fold. Should pharmacokinetic studies demonstrate a relatively short plasma half-life for this agent, this may suggest that optimal therapeutic effect could be achieved by maintaining blood concentrations of drug at therapeutic concentrations for at least 48 hrs. This could be achieved by frequent interval dosing or continuous infusion but may be important in the development of pre-clinical and clinical dosing strategies.

The antitumor effects of the $VEGF_{121}$/rGel fusion construct against both melanoma and human prostate carcinoma xenografts was impressive in magnitude and prolonged. A-375M and PC-3 cells in culture were resistant to the fusion construct *in vitro*, despite the reported presence of KDR on the melanoma (but not on PC-3) cells. Therefore, the antitumor effects observed *in vivo* appear not to be caused by direct cytotoxic effects of $VEGF_{121}$/rGel on the tumor cells themselves. The antitumor effect seems to be exerted indirectly on the tumor cells through specific damage to tumor vasculature. The $VEGF_{121}$ fusion toxin localized to tumor blood vessels after i.v. administration. Vascular damage and thrombosis of tumor blood vessels were observed within 48 h of administration of $VEGF_{121}$/rGel to PC-3 mice, consistent with the primary action of the construct being exerted on tumor vascular endothelium.

$VEGF_{121}$/rGel also has an impressive inhibitory effect on tumor metastases. Administration of the $VEGF_{121}$/rGel construct to mice previously injected (i.v.) with the MDA-MB-231 human breast tumor cells dramatically reduced

the number of tumor colonies found in lung, their size and their vascularity. In addition, the number of cycling breast tumor cells within lung metastatic foci was found to be reduced by an average of 60%. In addition to the reduced number of blood vessels present in lung metastases of treated mice, the few vessels present had a greatly reduced expression of VEGFR-2. Therefore, $VEGF_{121}$/rGel demonstrated an impressive, long-term impact on the growth and development of breast tumor metastatic foci found in lung.

The salient finding of the effects of $VEGF_{121}$/rGel construct is that this fusion toxin is specifically cytotoxic to cells over-expressing the KDR receptor for VEGF. However, the human breast MDA-MB-231 cancer cells employed for the metastatic studies described above do not express this receptor and, therefore, were not directly affected by this agent. The antitumor effects of $VEGF_{121}$/rGel observed on the MDA-MB-231 metastases thus appear to be solely the result of targeting tumor vasculature.

Neovascularization is a particularly important hallmark of breast tumor growth and metastatic spread. The growth factor VEGF-A and the receptor KDR have both been implicated in highly metastatic breast. It is of interest to note that administration of $VEGF_{121}$/rGel resulted in a 3-fold decrease in the number of Ki-67 labeled (cycling) cells in the metastatic foci present in lung (Figure 19). Clinical studies have suggested that tumor cell cycling may be an important prognostic marker for disease-free survival in metastatic breast cancer, but that Ki-67 labeling index, tumor microvessel density (MVD) and neovascularization appear to be independently regulated processes (Honkoop et al., 1998; Vartanian and Weidner, 1994). This is the first report of a significant reduction in tumor labeling index produced by a vascular targeting agent.

The vascular-ablative effects of the $VEGF_{121}$/rGel fusion construct alone were able to partially eradicate lung metastases. Although development of small, avascular, metastatic foci within lung tissue was observed, the growth of larger pulmonary metastases was completely inhibited by treatment with the $VEGF_{121}$/rGel fusion toxin. It is conceivable that combination of $VEGF_{121}$/rGel fusion construct with chemotherapeutic agents or with radiotherapeutic agents that directly damage tumor cells themselves may provide for greater therapeutic effect. Studies of several

vascular targeting agents in combination with chemotherapeutic agents have already demonstrated a distinct *in vivo* anti-tumor advantage of this combination modality against experimental tumors in mice (Siemann et al., 2002). Studies by Pedley et al. (2002) have also suggested that combination of vascular targeting and radioimmunotherapy may also present a potent antitumor combination. Finally, studies combining hyperthermia and radiotherapy with vascular targeting agents have demonstrated enhanced activity against mammary carcinoma tumors in mice (Murata et al., 2001).

EXAMPLE 24

Targeting Osteoclast Precursor Cells By $VEGF_{121}$/rGel

The present example shows that $VEGF_{121}$/rGel strongly inhibits the growth of prostate cancer cells PC-3 placed in the bone micro-environment in mice. Inhibition of tumor growth may not be solely due to targeting by $VEGF_{121}$/rGel of the tumor endothelium, but may also be due to targeting of osteoclast precursor cells. It is hypothesized that $VEGF_{121}$/rGel not only targets the tumor vasculature in the bone microenvironment but also prevents osteoclast maturation.

In a prostate cancer bone metastatic model, $VEGF_{121}$/rGel confers significant and impressive survival advantage on mice implanted with PC-3 prostate cancer cells in their femur (Figure 21). All control mice were sacrificed by day 67 due to large osteolytic lesions or bone lysis. In contrast, 50% of the $VEGF_{121}$/rGel-treated mice survived past day 140 without sign of osteolysis.

To further examine the effect of $VEGF_{121}$/rGel in the bone microenvironment, the effects of $VEGF_{121}$/rGel were examined in mouse myeloid cell line Raw 264.7, an osteoclast precursor cell. Treatment of Raw 264.7 cells with $VEGF_{121}$/rGel inhibited RANKL-mediated osteoclastogenesis (Figure 22). The observed effect was not mediated by either $VEGF_{121}$ or gelonin alone but was a characteristic unique to the combined fusion protein. Because data presented above indicate that the cytotoxicity of $VEGF_{121}$/rGel on endothelial cells is mediated through Flk-1/KDR and not Flt-1, it is hypothesized that Flk-1/KDR plays an important but as yet unknown role in RANKL-mediated osteoclastogenesis. It is also possible that

the biology of VEGF receptors is different in osteoclasts compared to endothelial cells, and $VEGF_{121}$/rGel is able to inhibit formation of osteoclasts via Flt-1.

Thus, $VEGF_{121}$/rGel may be targeting the tumor neovasculature as well as osteoclast precursor cells *in vivo*. This is significant because $VEGF_{121}$/rGel may inhibit prostate cancer osteoblastic lesions in bone as a result of osteoclastogenesis inhibition.

EXAMPLE 25

Determine the Effects of $VEGF_{121}$/rGel on Osteoclast Differentiation and Activation *in vitro*

The effects of $VEGF_{121}$/rGel on differentiation of osteoclast precursors can be examined in two *in vitro* model systems: (1) mouse osteoclast precursor cells RAW 264.7 that differentiate into mature osteoclasts upon stimulation with RANKL, and (2) bone marrow-derived macrophages that require stimulation with macrophage colony stimulating factor (MCSF) followed by RANKL for differentiation into osteoclasts. In both model systems, cells can be treated with $VEGF_{121}$/rGel, rGel, $VEGF_{121}$, or vehicle simultaneously with RANKL (or MCSF in the case of bone marrow-derived macrophages). Cells are allowed to differentiate for 4-5 days, followed by staining for tartrate-resistant acid phosphatase (TRAP). The dose-dependent effect of each protein can be quantitated by counting the number of TRAP-positive osteoclasts per well. Specificity of $VEGF_{121}$/rGel can be further tested by first treating the cells with increasing doses of $VEGF_{121}$ for one hour, followed by addition of $VEGF_{121}$/rGel or rGel, and monitoring for osteoclast formation.

To test if the effect of $VEGF_{121}$/rGel on osteoclastogenesis has functional significance, the effect of $VEGF_{121}$/rGel on bone resorption can be examined using experimental conditions as outlined above, except that the cells are plated on dentine. Six days after initiating osteoclast differentiation, the dentine will be examined for pits characteristic of bone resorption. Osteoclasts can be identified by TRAP-staining. The presence of bone-resorbing osteoclasts can also be observed *in vivo*. Relative resorptive area can be quantitated by reflective light microscopy.

It is hypothesized that the inhibition of RANKL-mediated osteoclastogenesis is due to cytotoxic effect of gelonin that enters the cells via the

targeted $VEGF_{121}$ receptors. This hypothesis can be tested by performing cytotoxicity assays on Raw 264.7 and bone marrow-derived macrophages with $VEGF_{121}$/rGel and rGel using crystal violet staining as previously described, and determine the IC_{50} for each drug. A lower IC_{50} for $VEGF_{121}$/rGel than rGel alone will confirm that $VEGF_{121}$ is important in the specific targeting of these cells. If a cytotoxic effect of $VEGF_{121}$/rGel on Raw 264.7 cells is observed, the mechanism of cell death can be investigated by TUNEL assay and examining caspase-3 cleavage, PARP cleavage as well as changes in cytochrome c, Bax, Bcl and Bcl-xl levels.

EXAMPLE 26

Cloning of Human Granzyme B Gene And Construction of Granzyme B/$VEGF_{121}$ Fusion Gene

The following examples describe a fusion construct of $VEGF_{121}$ and proapoptotic enzyme granzyme B (GrB) designed for specific delivery to tumor neovasculature. Human granzyme B gene was cloned from human cutaneous T-cell lymphoma (HuT-78) cells and then fused to $VEGF_{121}$ via a short, flexible tether using a PCR-based construction method. The fusion protein was expressed in *Escherichia coli* and purified by nickel-NTA metal affinity chromatography. The fusion protein GrB/$VEGF_{121}$ was characterized and the biological activities and mechanism were determined.

RNA from HuT-78 cells was isolated and target premature human granzyme B cDNA was amplified by reverse transcription-PCR using the following primers: NcoIgb, 5'-GGTGGCGGTGGCTCCATGGAACCAATCCTGCTTCTG-3' (SEQ ID NO. 5) and CxhoIgb, 5'-GCCACCGCCTCCCTCGAGCTATTAGTAGCGTTTCATGGT-3' (SEQ ID NO. 6). The human granzyme B sequence with signal sequence was designated as premature granzyme B (~800 bp) (Figure 23). The PCR product was then cloned into the PCR 2.1 TA vector designated as gbTA. The gbTA was transformed into INVaF' competent cells, and positive clones were screened by PCR. The DNA from positive clones was isolated and then sequenced. The correct clone was designated gbTA-2.

In cytotoxic cells, active granzyme B was generated from a zymogen by dipeptidyl peptidase I-mediated proteolysis, which removes the two residue (Gly-

Glu), propeptide and exposes Ile^{21}. The amino-terminal Ile-Ile-Gly-Gly sequence of granzyme B is necessary for the mature, active granzyme B.

To construct $GrB/VEGF_{121}$ fusion gene, the coding sequence of granzyme B was amplified by PCR from Ile^{21}, effectively deleting the signal sequence and Gly-Glu domain. At the same time, a cleavage site for EK (DDDDK, SEQ ID NO. 7) was inserted upstream and adjacent to Ile^{21}. Mature granzyme B was attached to the recombinant $VEGF_{121}$ carrier via flexible tether (G_4S). The fused gene fragment was then introduced into the *Xba*I and *Xho*I sites of the pET32a(+) to form the expression vector $pET32GrB/VEGF_{121}$ (Figure 24). This vector contains a T7 promoter for high-level expression followed by a Trx.tag, a His.tag, a thrombin cleavage site, and an EK cleavage site for final removal of the protein purification tag. Once protein tag is removed by rEK digestion, the first residue (isoleucine) of mature granzyme B is exposed, thereby activating the granzyme B moiety of $GrB/VEGF_{121}$ construct.

The $GrB/VEGF_{121}$ fusion gene was constructed by an overlap PCR method. Briefly, granzyme B coding sequence was amplified from gbTA-2 using the following primers: NgbEK, 5'-GGTACCGACGACGACGACAAGATCATCGGGGGACATGAG-3' (SEQ ID NO. 8) and Cgb, 5'-GGAGCCACCGCCACCGTAGCGTTTCATGGT-3' (SEQ ID NO. 9). These were designed to delete the signal sequence of premature granzyme B, insert an EK cleavage site at the amino terminus, and add a G4S linker sequence to the carboxyl terminus to serve as a link to the $VEGF_{121}$ gene. $VEGF_{121}$ sequence was amplified from a plasmid $pET22\text{-}VEGF_{121}$ (from Dr. Philip Thorpe, University of Texas Southwestern Medical Center, Dallas, TX) using the following primers: Nvegf, 5'-GGTGGCGGTGGCTCCGCACCCATGGCAGAA-3' (SEQ ID NO. 10) and CxhoIveg, 5'-AAGGCTCGTGTCGACCTCGAGTCATTACCGCCTCGGCTTGTC-3' (SEQ ID NO. 11). To clone the fused genes into pET32a(+) vector with an EK site at the amino terminus of granzyme B, the fragment from pET32a(+) was amplified using the following primers: T7 promoter, 5'-TAATACGACTCACTATAG (SEQ ID NO. 12) and CpET32EK, 5'-CTTGTCGTCGTCGTCGGTACCCAGATCTGG-3' (SEQ ID NO. 13). The primer has an EK site at carboxyl terminus overlapping with the amino

terminus of the fused gene. Using overlap PCR, the fusion genes (EK-GrB/$VEGF_{121}$) were constructed using as primers the T7 promoter and CxhoI veg. Amplified fragments were purified, digested with *Xba*I and *Xho*I, and cloned into pET32a(+) vector, designed as pET32GrB/$VEGF_{121}$. A correct clone was chosen for transformation into AD_{494} (DE_3) pLysS-competent cells for further induction and expression.

EXAMPLE 27

Expression And Purification of Granzyme B/$VEGF_{121}$ Fusion Protein

Bacterial colonies transformed with the constructed plasmid were grown in Luria broth medium (containing 400 mg/ml carbenicillin, 70 mg/ml chloramphenicol, and 15 mg/ml kanamycin) at 37°C overnight at 240 rpm in a shaking incubator. The cultures were then diluted 1:100 in fresh Luria broth + antibiotics (200 mg/ml ampicillin, 70 mg/ml chloramphenicol, and 15 mg/ml kanamycin) and grown to A_{600nm} = 0.6 at 37°C; thereafter, isopropyl-1-thio-b-D-galactopyranoside was added to a final concentration of 100 mM and the cells were incubated at 37°C for 2 h to induce fusion protein expression. The cells were harvested, resuspended in 10 mM Tris (pH 8.0), and stored frozen at -80^{0}C for later purification.

Thawed, resuspended cells were lysed by addition of lysozyme to a final concentration of 100 mg/ml with agitation for 30 min at 4^{0}C followed by sonication. Extracts were centrifuged at 186,000 x g for 1 h. The supernatant containing only soluble protein was adjusted to 40 mM Tris, 300 mM NaCl, and 5 mM imidazole (pH 8.0) and applied to nickel-NTA agarose resin equilibrated with the same buffer. The nickel-NTA agarose was washed with 300 mM NaCl and 20 mM imidazole and the bound proteins were eluted with 500 mM NaCl and 500 mM imidazole. Absorbance (280 nm) and SDS-PAGE analyses were performed to determine the presence of the polyhistidine-tagged protein, designated as Pro-GrB/$VEGF_{121}$. The eluted Pro-GrB/$VEGF_{121}$ was dialyzed against 20 mM Tris-HCl (pH 7.4) and 150 mM NaCl. The GrB moiety of Pro-GrB/$VEGF_{121}$ was activated by the addition of bovine rEK to remove the polyhistidine tag according to the manufacturer's instructions (1 unit of rEK for cleavage of 50 mg protein incubated at room temperature for 16 h). The rEK was removed by EK capture agarose. The

protein solution was then passed through a column containing Q-Sepharose to remove non-rEK-digested construct and nonspecific proteins. The product was analyzed by SDS-PAGE to determine purity, and Bio-Rad protein assay was used to determine protein concentration. Samples were then aliquoted and stored at 4^0C.

One liter of the culture typically yielded ~100 mg of the final purified GrB/$VEGF_{121}$ product. SDS-PAGE analysis showed that the final purified GrB/$VEGF_{121}$ fusion construct migrated under reducing conditions as a band at the expected molecular mass of 38 kDa (Figure 25A). Specificity of the cleaved fusion protein was confirmed by Western blot using either VEGF121 mouse monoclonal antibody or GrB mouse monoclonal antibody (Figure 25B).

EXAMPLE 28

Binding Activity of Granzyme B/$VEGF_{121}$ Fusion Protein

Binding activity of GrB/$VEGF_{121}$ was determined by ELISA. Ninety six-well plates coated with 50,000 cells/well of PAE/FLK-1, PAE/FLT-1, human melanoma A375M or human breast cancer SKBR3-HP cells were blocked by 5% BSA and then treated with purified GrB/$VEGF_{121}$ at various concentrations. After washing, the plates were incubated with either GrB antibody or $VEGF_{121}$ antibody followed by HRP-goat anti-mouse IgG. Then, the substrate 2,2'-azino-bis-3-ethylbenzthiazoline-6-sulfonic acid (ABTS) solution with 1 ml/ml of 30% H_2O_2 was added to the wells. Absorbance at 405 nm was measured after 30 min.

GrB/$VEGF_{121}$ specifically bound to PAE/FLK-1 cells. However, the protein did not bind to PAE/FLT-1 cells or to melanoma A375M or human breast cancer SKBR3-HP cells, as detected by either an anti-GrB mouse monoclonal antibody (Figure 26A) or an anti-$VEGF_{121}$ mouse monoclonal antibody (Figure 26B).

EXAMPLE 29

Internalization of Granzyme B/$VEGF_{121}$ Fusion Protein Assessed By Immunofluorescence Microscopy

Cells were plated in 16-well chamber slides (Nunc, Nalge Nunc International, Naperville, IL) at 1 x 10^4 cells/well and incubated overnight at 37^0C in a 5% CO_2 air atmosphere. Cells were treated with 100 nM of GrB/$VEGF_{121}$ for 4 h and

then washed briefly with PBS. The cell surface was stripped by incubation with glycine buffer (500 mM NaCl, 0.1 M glycine [pH 2.5]) and neutralized for 2 min with 0.5 M Tris (pH 7.4) followed by wash with PBS. Cells were fixed in 3.7% formaldehyde for 15 min at room temperature, permeabilized for 10 min in PBS containing 0.2% Triton X-100 and washed thrice with PBS. Samples were incubated with 3% BSA for 1 h at room temperature to block nonspecific binding sites before incubating with anti-GrB mouse monoclonal antibody (1:100 dilution) at room temperature for 1 h followed by incubation with FITC-coupled anti-mouse IgG (1:100 dilution) at room temperature for 1 h. The walls and gaskets of the chamber slide were then removed carefully. After air drying, the slide was mounted and analyzed under a Nikon Eclipse TS-100 fluorescence microscope. Photographs were taken with a scope-mounted camera.

Immunofluorescent staining clearly showed that the GrB moiety of GrB/$VEGF_{121}$ was delivered into the cytosol of PAE/FLK-1 but not into that of PAE/FLT-1 cells after treatment with GrB/$VEGF_{121}$ for 4 h (Figure 27). Analysis of PAE/FLK-1 cells treated for 24 and 48 h demonstrated no further increase in immunofluorescent staining over that observed at 4 h.

EXAMPLE 30

Cytotoxicity of Granzyme B/$VEGF_{121}$ Fusion Protein

The cytotoxicity of GrB/$VEGF_{121}$ was assessed against log-phase PAE/FLK-1 and PAE/FLT-1 cells in culture. PAE cells in Ham's F-12 medium with 10% fetal bovine serum were plated into 96-well plates at a density of 2.5 x 10^3 cells/well and allowed to adhere for 24 h at 37^0C in 5% CO_2. After 24 h, the medium was replaced with medium containing different concentrations of GrB/$VEGF_{121}$ or $VEGF_{121}$/rGel. After 72 h, the effect of GrB/$VEGF_{121}$ or $VEGF_{121}$/rGel on the growth of cells in culture was determined using 2,3-bis[2-methoxy-4-nitro-5-sulfophenyl]-2H-tetrazolium-5-carboxanilide inner salt (XTT). Plates were read on a microplate ELISA reader at 540 nm.

An IC_{50} effect was found at a concentration of ~10 nM on PAE/FLK-1 cells. However, no cytotoxic effects were found on PAE/FLT-1 cells at doses up to 200 nM (Figure 28A). By comparison, the cytotoxic effects of another fusion toxin,

$VEGF_{121}$/rGel, were relatively greater (on a molar basis) against target cells in culture and demonstrated specific cytotoxicity against PAE/FLK-1 cells at an IC_{50} of ~1 nM.

The growth inhibitory effects of GrB/$VEGF_{121}$ on the proliferation of PAE cells were evaluated by clonogenic assay. Briefly, 5 x 10^5 PAE cells/ml were incubated at 37°C and 5% CO_2 for 72 h with different concentrations of either GrB/$VEGF_{121}$ or 100 nM of irrelevant fusion protein GrB/scFvMEL. Cells were then washed with PBS, trypsinized, counted by hemacytometer, and diluted serially. The serial cell suspensions were then plated in triplicate and cultured in six-well plates for 5–7 days. Cells were stained with crystal violet and colonies consisting of >20 cells were counted using an inverted light microscope. Growth inhibition was defined as the percentage of cell growth/number of colonies in treated samples in relation to that in the nontreated control sample.

In the clonogenic assay (Figure 28B), the concentration of GrB/$VEGF_{121}$ which suppressed cell colony growth by 50% (IC_{50}) was determined to be ~20 nM on PAE/FLK-cells. In contrast, there was no effect on colony growth of PAE/FLT-1 cells at concentrations of GrB/$VEGF_{121}$ up to 100 nM. There was also no effect of irrelevant fusion protein GrB/scFvMEL targeting human melanoma cells on colony growth of PAE cells at concentrations of 100 nM.

EXAMPLE 31

In Situ Cell Death Detection (TUNEL Assay)

Cleavage of genomic DNA during apoptosis may yield double-stranded, low molecular mass DNA fragments as well as single-strand breaks (nicks) in high molecular mass DNA. The DNA strand breaks can be identified by labeling free 3' hydroxyl termini with modified nucleotides in an enzymatic reaction. Cells (1 x 10^4 cells/well) were treated with GrB/$VEGF_{121}$ at the IC_{50} concentration for different times (24 and 48 h) and washed briefly with PBS. Cells were fixed with 3.7% formaldehyde at room temperature for 20 min, rinsed with PBS, permeablized with 0.1% Triton X-100, 0.1% sodium citrate on ice for 2 min, and washed with PBS twice. Cells were incubated with TUNEL reaction mixture at 37°C for 60 min followed by incubation with Converter-AP at 37°C for 30 min and finally treated with Fast Red substrate solution at room temperature for 10 min. After the final wash

step, the slides were mounted and analyzed for nucleus staining of apoptotic cells under a light microscope with 400x magnification.

TUNEL assay produced positive results on GrB/$VEGF_{121}$-treated PAE/FLK-1 cells at 24 h (75%) and 48 h (85%) but not on GrB/$VEGF_{121}$-treated PAE/FLT-1 cells (10%) (Figure 29), indicating that GrB/$VEGF_{121}$ induced apoptosis in PAE/FLK-1 cells.

EXAMPLE 32

Cytochrome c Release Assay And Bax Translocation

PAE cells (5×10^7) were treated with GrB/$VEGF_{121}$ at concentrations of 0.1 and 20 nM for 24 h. After cells were washed with 10 ml of ice-cold PBS, they were resuspended with 0.5 ml of 1x cytosol extraction buffer mix containing DTT and protease inhibitors and incubated on ice for 10 min. Cells were homogenized in an ice-cold glass homogenizer. The homogenate was centrifuged at 700 x g for 10 min at 4^0C. The supernatant was transferred to a fresh 1.5 ml tube and centrifuged at 10,000 x g for 30 min at 4^0C. The supernatant was collected and labeled as cytosolic fraction. The pellet was resuspended in 0.1 ml mitochondrial extraction buffer mix containing DTT and protease inhibitors, vortexed for 10 s, and saved as mitochondrial fraction. Protein concentrations were determined by using Bio-Rad Bradford protein assay. Aliquots of 30 mg from each cytosolic and mitochondrial fraction isolated from non-treated and treated cells were loaded on a 15% SDS-PAGE. Standard Western blot procedure was performed, and the blot was probed with mouse anti-cytochrome c antibody (1 mg/ml) or mouse anti-Bax antibody (1 mg/ml).

Western blot studies demonstrated that cytochrome c was released from mitochondria into the cytosol after treating PAE/FLK-1 cells with 20 nM GrB/$VEGF_{121}$, but this effect was not observed on PAE/FLT-1 cells (Figure 30). Bax was found to be normally present in both cytosol and mitochondria of untreated PAE cells. However, when PAE/FLK-1 cells were treated with 20 nM of GrB/$VEGF_{121}$, Bax levels decreased in cytosol and increased in mitochondria. This effect was not observed on PAE/FLT-1 cells (Figure 30).

EXAMPLE 33

Granzyme B/$VEGF_{121}$ Induces DNA Laddering

PAE cells were plated onto six-well plates (2 x 10^5 cells/well). Twenty-four hours later, cells were shifted to fresh culture medium containing 20 nM of GrB/$VEGF_{121}$ (1.5 ml/well). After 24 h of incubation at 37^0C, DNA was extracted and purified with DNA ladder kit (Roche) and fractionated on 1.5% agarose gels.

DNA laddering indicative of apoptosis was observed after a 24-h exposure with GrB/$VEGF_{121}$ on PAE/FLK-1 cells. As expected, there was no DNA laddering detected on PAE/FLT-1 cells after treatment with the fusion construct (Figure 31).

EXAMPLE 34

Granzyme B/$VEGF_{121}$ Activates Caspases On Porcine Aortic Endothelial Cells

PAE cells were treated with GrB/$VEGF_{121}$, total cell lysates were loaded onto 12% SDS-PAGE, and standard Western blotting was performed. Treatment with GrB/$VEGF_{121}$ cleaved caspase-8, caspase-3, and PARP on PAE/FLK-1 cells but not on PAE/FLT-1 cells (Fig 32). These data indicate that the GrB/$VEGF_{121}$ construct activated caspases involved in the apoptosis pathway.

The following references were cited herein:

Brekken, et al., Cancer Res. 58:1952–1959 (1998).

Honkoop et al., Br. J. Cancer 77:621-26 (1998).

Murata et al., Int. J. Radiat. Oncol. Biol. Phys. 51:1018-24 (2001).

Pedley et al., Int. J. Radiat. Oncol. Biol. Phys. 54:1524-31 (2002).

Siemann et al., Int. J. Cancer 99:1-6 (2002).

Vartanian and Weidner, Am. J. Pathol. 144:1188-94 (1994).

Veenendaal et al., Proc Natl Acad Sci USA 99:7866-71 (2002).

Any patents or publications mentioned in this specification are indicative of the levels of those skilled in the art to which the invention pertains. Further, these patents and publications are incorporated by reference herein to the same extent as if each individual publication was specifically and individually indicated to be incorporated by reference.

WHAT IS CLAIMED IS:

1. A conjugate comprising the 121-amino acid isoform of vascular endothelial growth factor ($VEGF_{121}$) and a cytotoxic molecule.

2. The conjugate of claim 1, wherein said conjugate is a fusion protein of $VEGF_{121}$ and said cytotoxic molecule.

3. The conjugate of claim 1, wherein said cytotoxic molecule is a toxin or a signal transduction protein capable of generating apoptotic signals.

4. The conjugate of claim 3, wherein said toxin is gelonin.

5. The conjugate of claim 3, wherein said signal transduction protein capable of generating apoptotic signals is granzyme B or Bax.

6. The conjugate of claim 1, wherein said $VEGF_{121}$ and said cytotoxic molecule are linked by a linker selected from the group consisting of G_4S, $(G_4S)2$, 218 linker, $(G_4S)3$, enzymatically cleavable linker and pH cleavable linker.

7. A pharmaceutical composition comprising the conjugate of claim 1.

8. A method of killing a cell expressing type 2 vascular endothelial growth factor receptor (kinase domain receptor/Flk-1 receptor), comprising the steps of:

contacting said cell with a pharmacologically effective amount of a conjugate comprising the 121-amino acid isoform of vascular endothelial growth factor ($VEGF_{121}$) and a cytotoxic molecule.

9. The method of claim 8, wherein said cytotoxic molecule is a toxin or a signal transduction protein capable of generating apoptotic signals.

10. The method of claim 8, wherein said conjugate is a fusion protein comprising $VEGF_{121}$ and gelonin or a fusion protein comprising $VEGF_{121}$ and granzyme B or Bax.

11. The method of claim 8, wherein said $VEGF_{121}$ and said cytotoxic molecule are linked by a linker selected from the group consisting of G_4S, $(G_4S)2$, 218 linker, $(G_4S)3$, enzymatically cleavable linker and pH cleavable linker.

12. The method of claim 8, wherein said conjugate is cytotoxic to cells expressing more than 2000 type 2 VEGF receptors per cell.

13. A method of inhibiting tumor growth or inhibiting metastatic spread and vascularization of metastases in a subject, comprising the step of administering to said subject a biologically effective amount of a conjugate capable of exerting a cytotoxic effect on the tumor vasculature, said conjugate comprises the 121-amino acid isoform of vascular endothelial growth factor ($VEGF_{121}$) and a cytotoxic molecule, wherein said $VEGF_{121}$ binds to both VEGF receptor type 1 (Flt-1) and VEGF receptor type 2 (kinase domain receptor/Flk-1) but is only internalized by cells expressing VEGF receptor type 2.

14. The method of claim 13, wherein said cytotoxic molecule is a toxin or a signal transduction protein capable of generating apoptotic signals.

15. The method of claim 13, wherein said conjugate is a fusion protein comprising $VEGF_{121}$ and gelonin or a fusion protein comprising $VEGF_{121}$ and granzyme B or Bax.

16. The method of claim 13, wherein said $VEGF_{121}$ and said cytotoxic molecule are linked by a linker selected from the group consisting of G_4S, $(G_4S)3$, $(G_4S)2$, 218 linker, enzymatically cleavable linker and pH cleavable linker.

17. The method of claim 13, wherein said conjugate is cytotoxic to cells expressing more than 2000 type 2 VEGF receptors per cell.

18. The method of claim 13, further comprises treatment with chemotherapeutic agents or radiotherapeutic agents.

19. A method of inhibiting osteoclastogenesis or treating osteoporosis in a subject, comprising the step of administering to said subject a biologically effective amount of a conjugate comprising the 121-amino acid isoform of vascular endothelial growth factor ($VEGF_{121}$) and a cytotoxic molecule.

20. The method of claim 19, wherein said cytotoxic molecule is a toxin or a signal transduction protein capable of generating apoptotic signals.

21. The method of claim 19, wherein said conjugate is a fusion protein comprising $VEGF_{121}$ and gelonin or a fusion protein comprising $VEGF_{121}$ and granzyme B or Bax.

22. The method of claim 19, wherein said $VEGF_{121}$ and said cytotoxic molecule are linked by a linker selected from the group consisting of G_4S, $(G_4S)2$, 218 linker, $(G_4S)3$, enzymatically cleavable linker and pH cleavable linker.

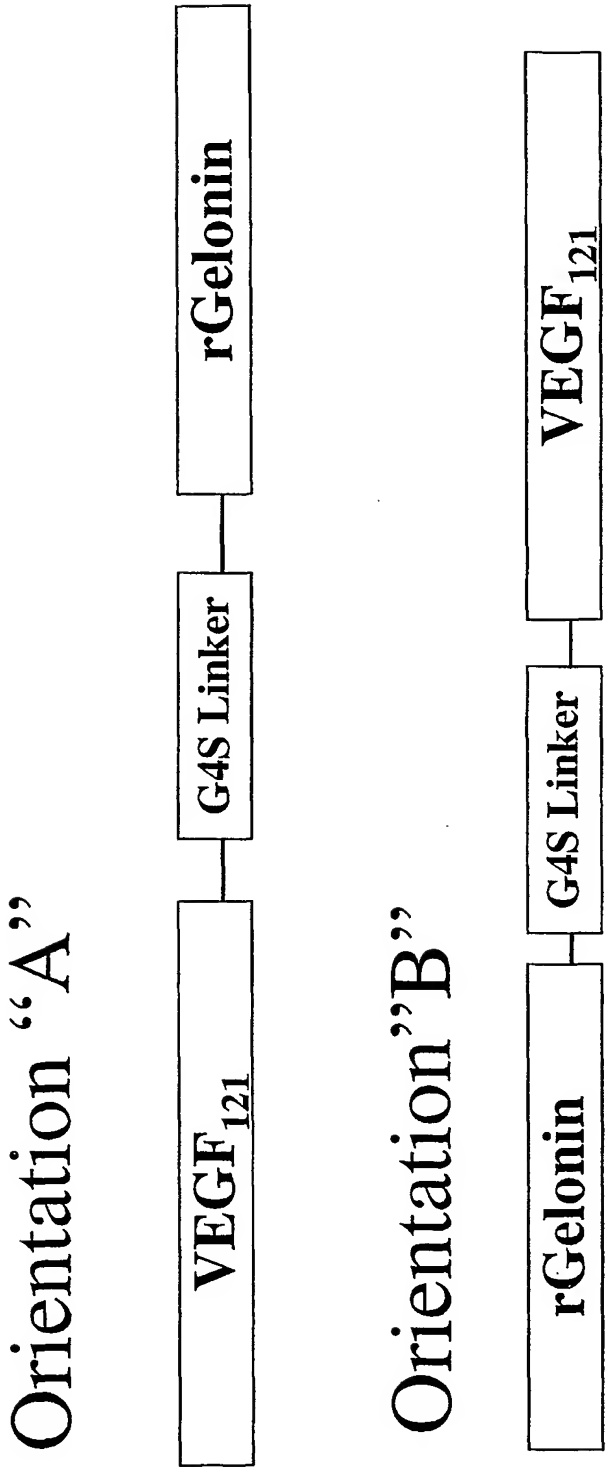
Orientation "A"
VEGF121
G4S Linker
rGelonin
Orientation"B"
rGelonin
G4S Linker
VEGF121

Fig. 1

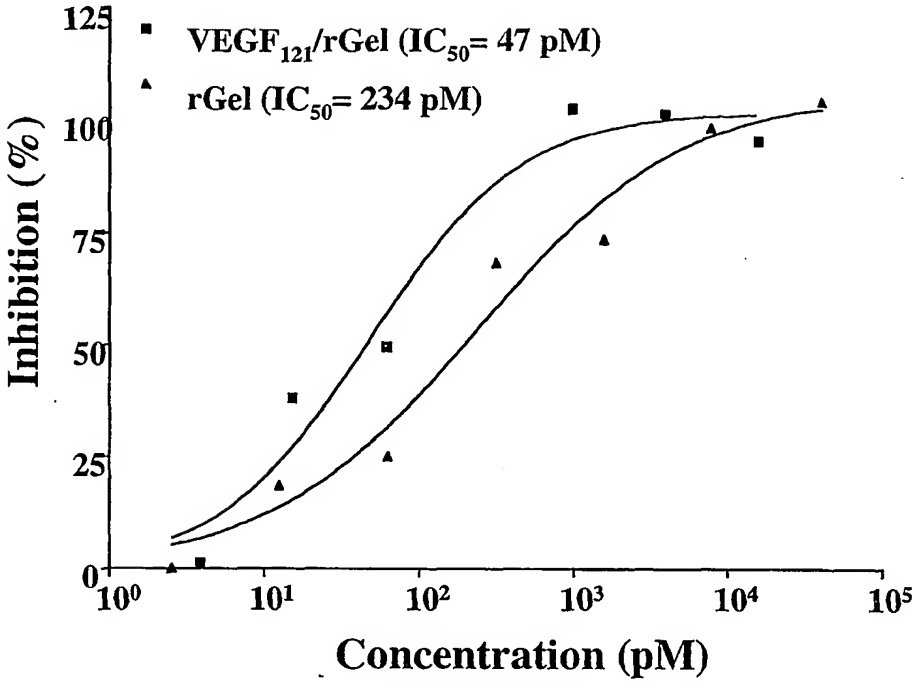
VEGF121/rGel (IC50= 47 pM)
rGel (IC50= 234 pM)
Inhibition (%)
125
100
75
50
25
0
10^0
10^1
10^2
10^3
10^4
10^5
Concentration (pM)

Fig. 2

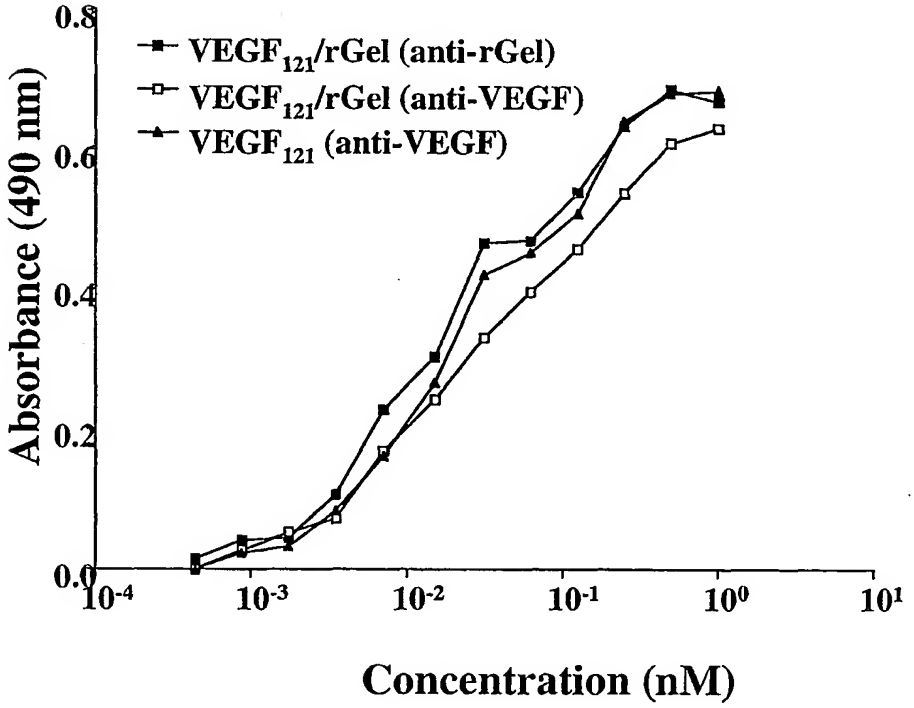
VEGF121/rGel (anti-rGel)
VEGF121/rGel (anti-VEGF)
VEGF121 (anti-VEGF)
Absorbance (490 nm)
0.8
0.6
0.4
0.2
0.0
10-4
10-3
10-2
10-1
10^0
10^1
Concentration (nM)

Fig. 3

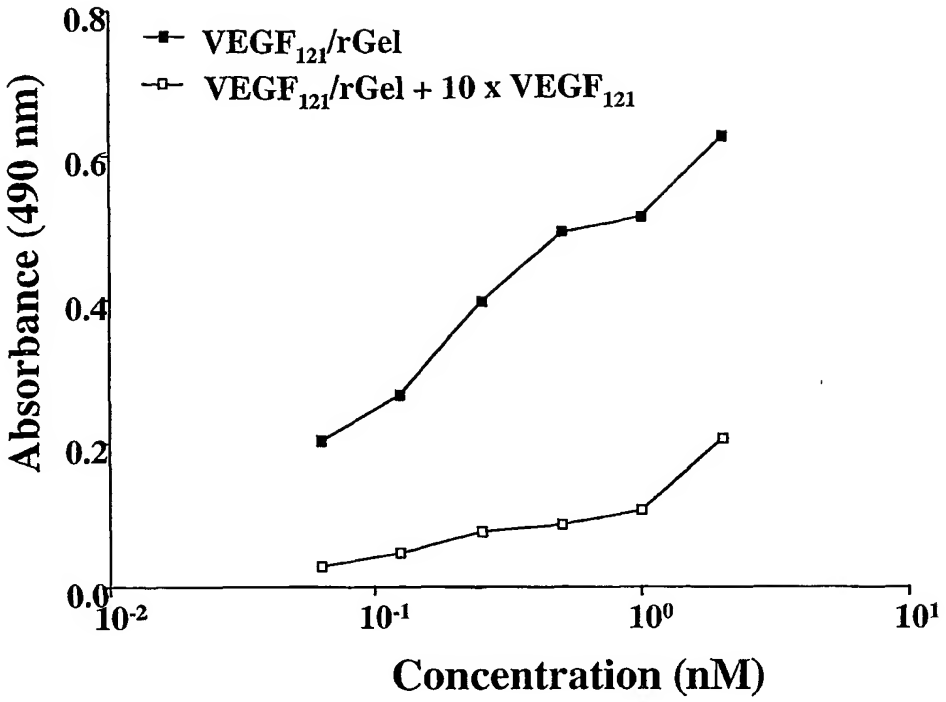
VEGF121/rGel
VEGF121/rGel + 10 x VEGF121
Absorbance (490 nm)
0.8
0.6
0.4
0.2
0.0
10-2
10-1
100
101
Concentration (nM)

Fig. 4

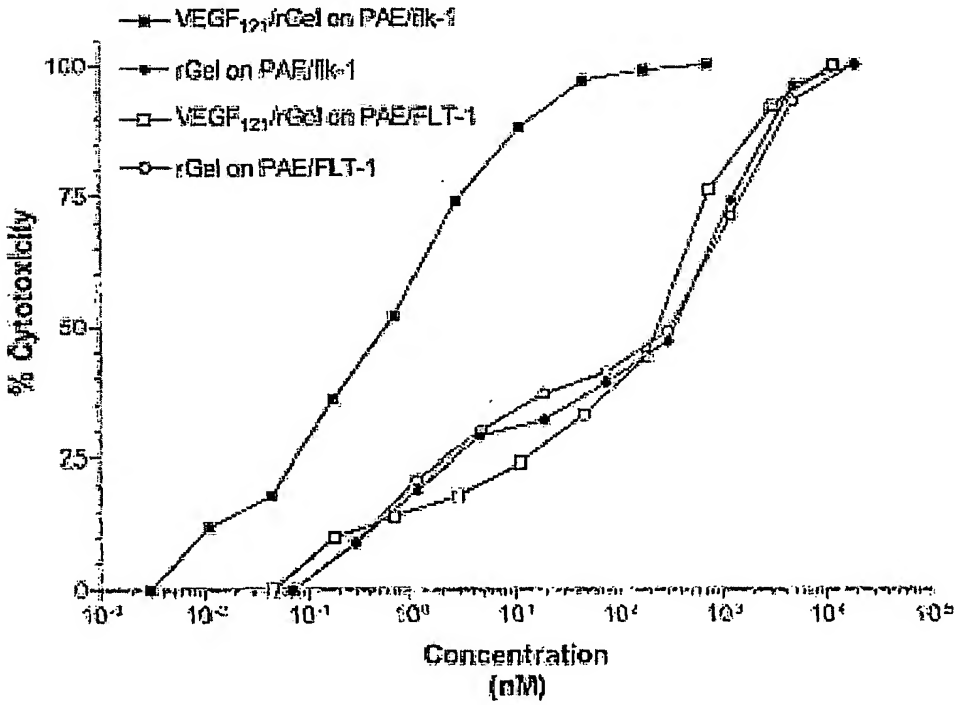
VEGF121/rGel on PAE/flk-1
rGel on PAE/flk-1
VEGF121/rGel on PAE/FLT-1
rGel on PAE/FLT-1
% Cytotoxicity
100
75
50
25
0
Concentration (nM)

Fig. 5

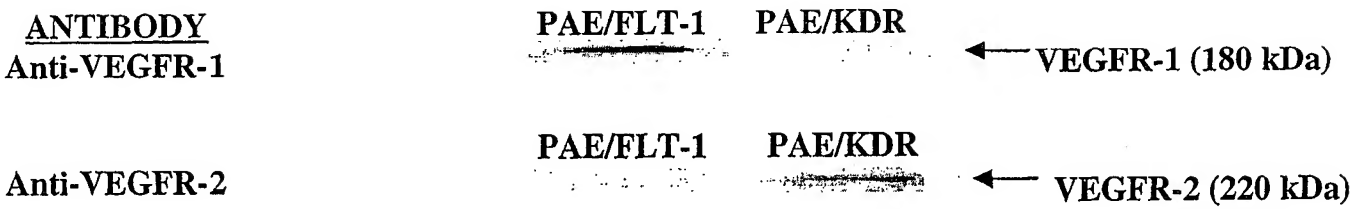
ANTIBODY
Anti-VEGFR-1
PAE/FLT-1
PAE/KDR
VEGFR-1 (180 kDa)
Anti-VEGFR-2
PAE/FLT-1
PAE/KDR
VEGFR-2 (220 kDa)

Fig. 6A

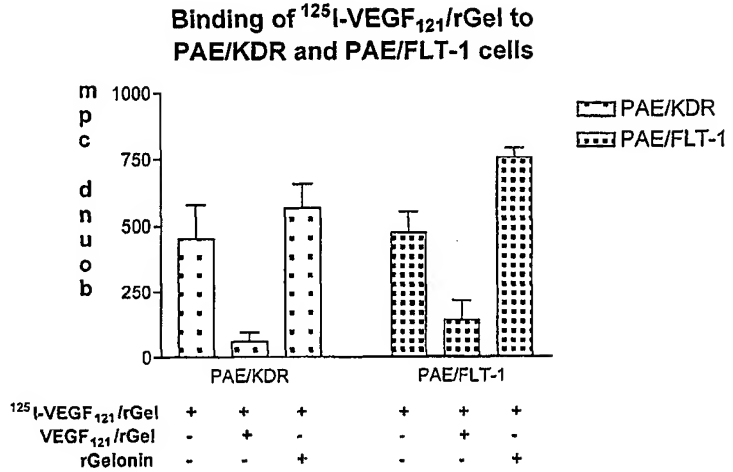
Binding of 125I-VEGF121/rGel to
PAE/KDR and PAE/FLT-1 cells
cpm bound
1000
750
500
250
0
PAE/KDR
PAE/FLT-1
125I-VEGF121/rGel + + + + + +
VEGF121/rGel - + - - + -
rGelonin - - + - - +

Fig. 6B

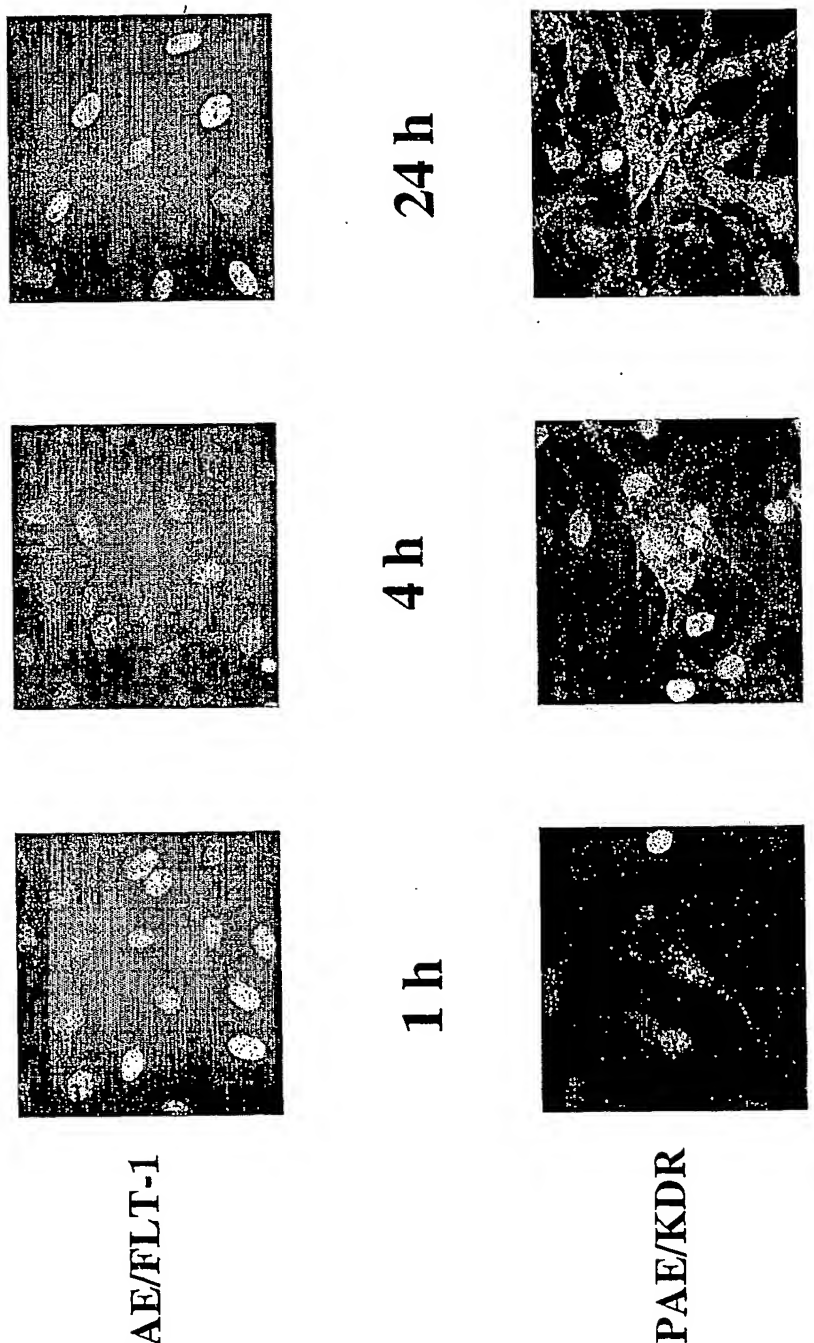

Fig. 7

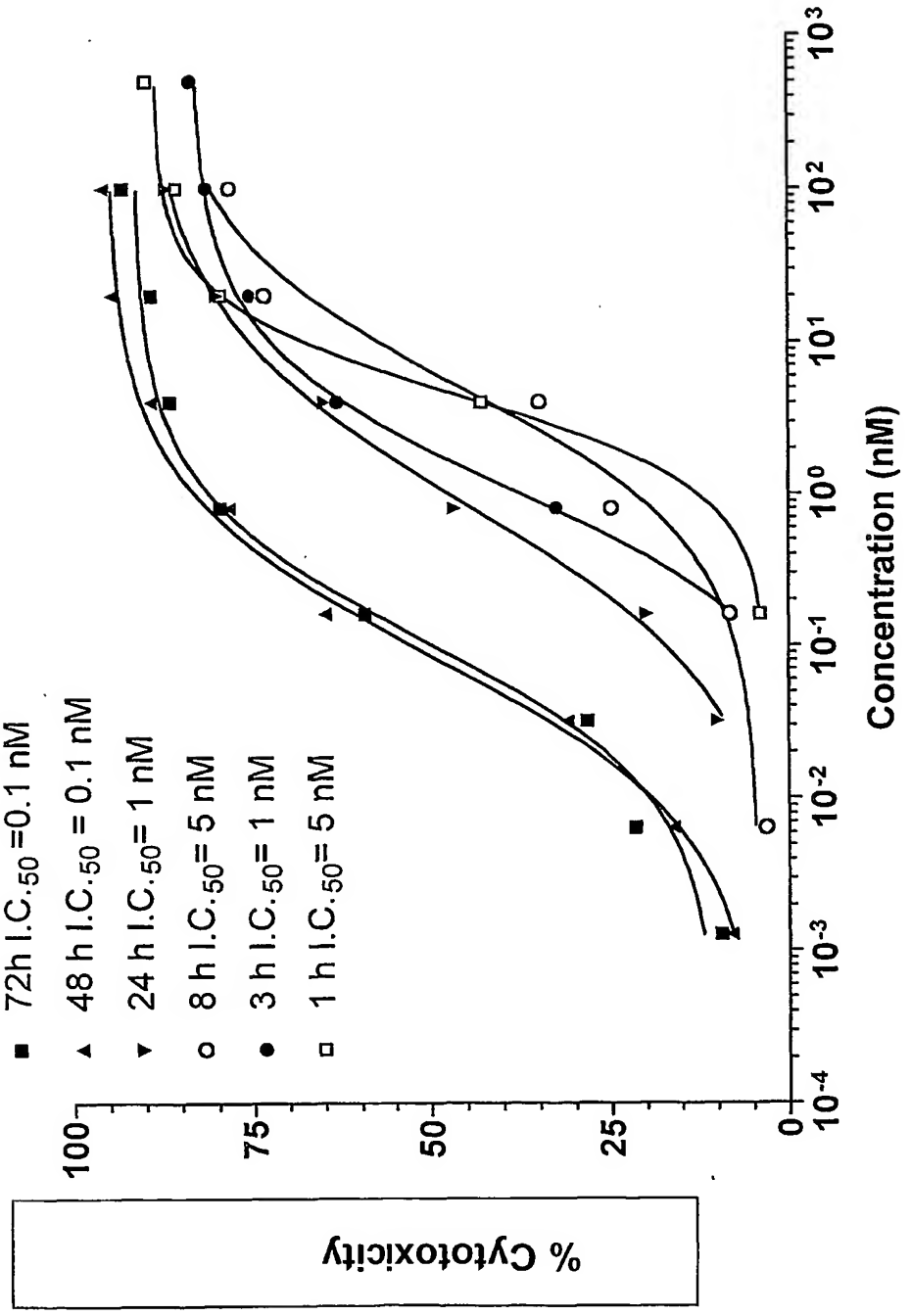
% Cytotoxicity
100
75
50
25
0
10^{-4}
10^{-3}
10^{-2}
10^{-1}
10^{0}
10^{1}
10^{2}
10^{3}
Concentration (nM)
72h I.C.$_{50}$ =0.1 nM
48 h I.C.$_{50}$ = 0.1 nM
24 h I.C.$_{50}$= 1 nM
8 h I.C.$_{50}$= 5 nM
3 h I.C.$_{50}$= 1 nM
1 h I.C.$_{50}$= 5 nM

Fig. 8

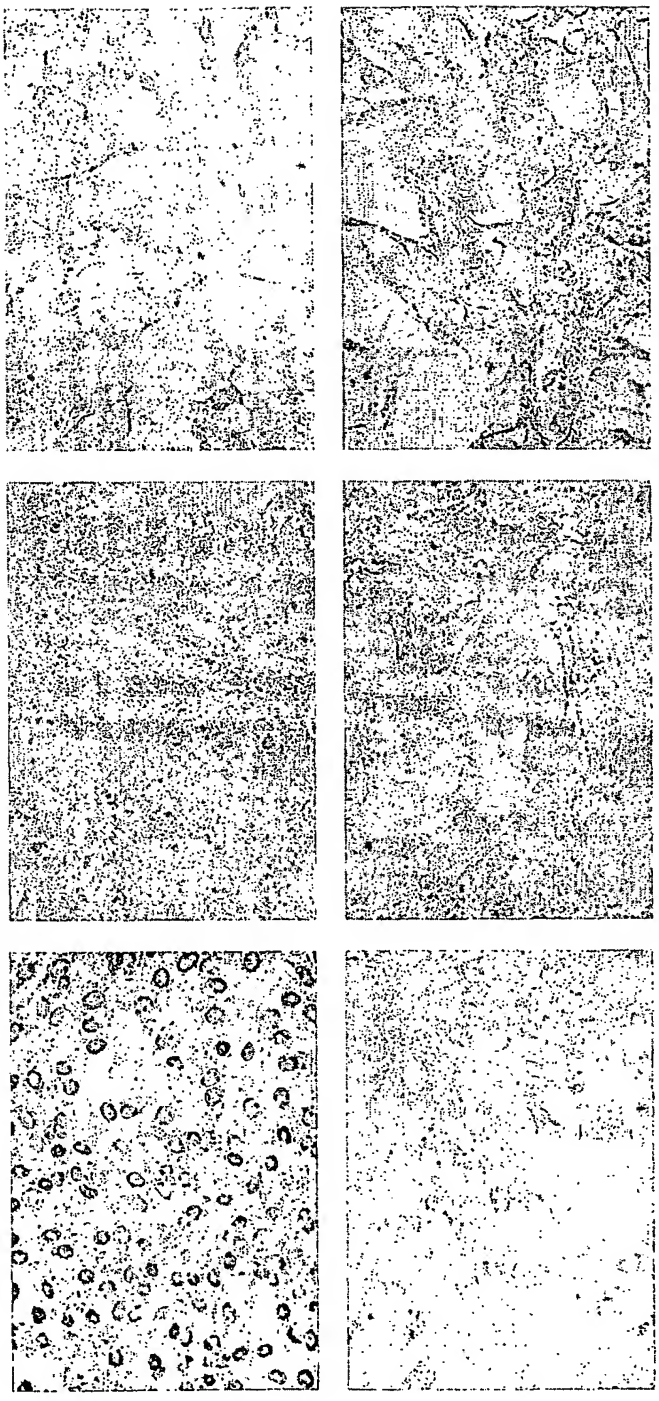

Fig. 9

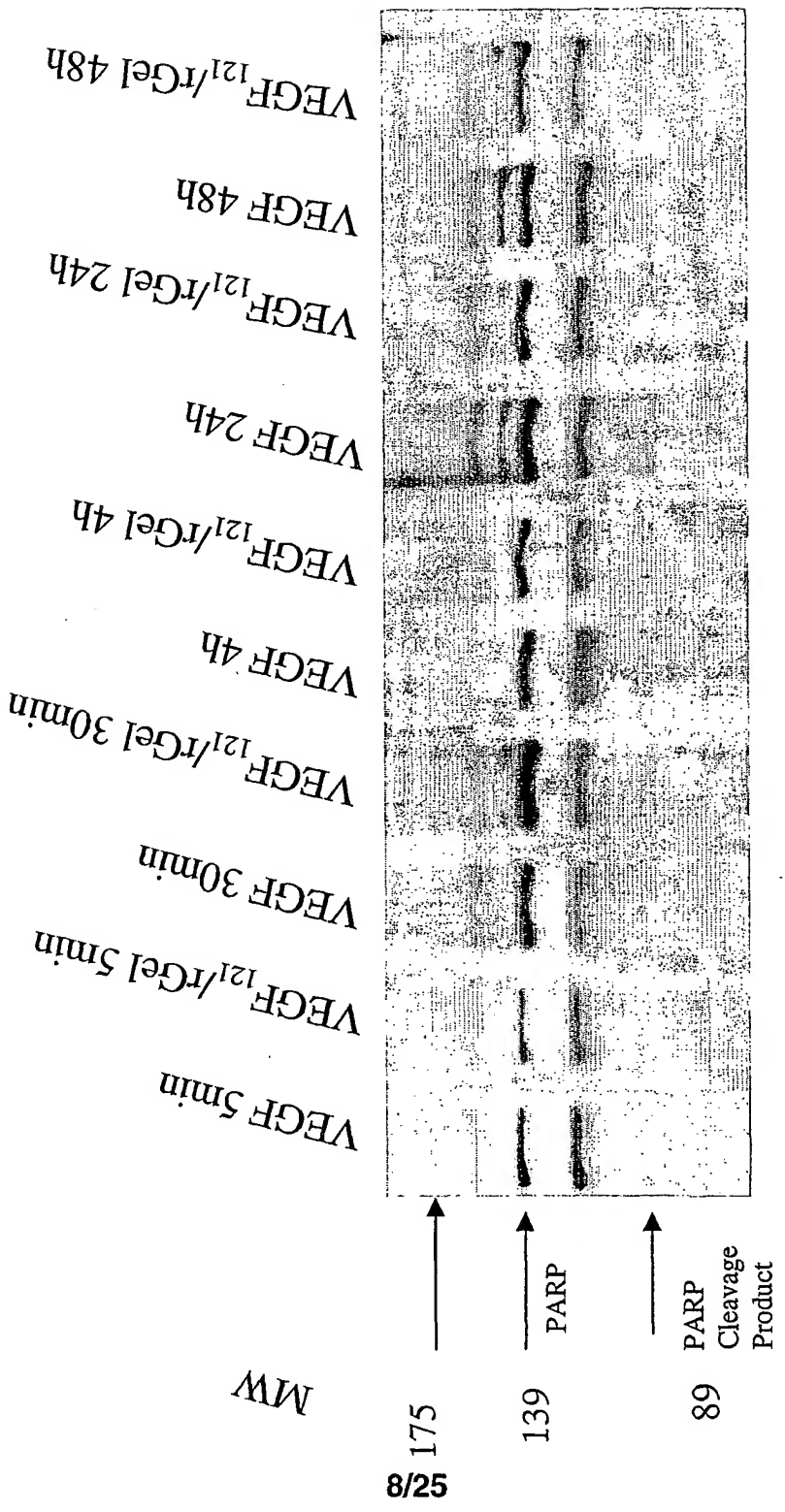
MW
175
139
89
PARP
PARP Cleavage Product
VEGF 5min
VEGF121/rGel 5min
VEGF 30min
VEGF121/rGel 30min
VEGF 4h
VEGF121/rGel 4h
VEGF 24h
VEGF121/rGel 24h
VEGF 48h
VEGF121/rGel 48h

Fig. 10

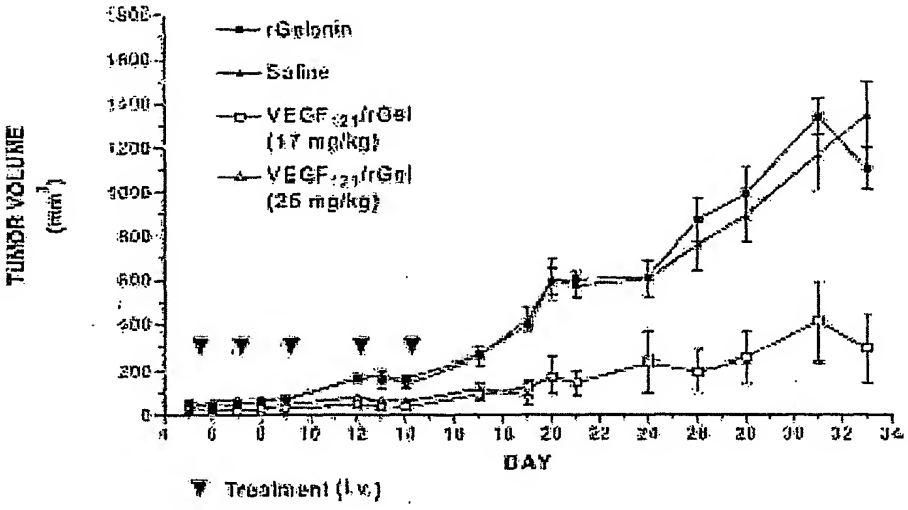
rGelonin
Saline
VEGF121/rGel (17 mg/kg)
VEGF121/rGel (26 mg/kg)
TUMOR VOLUME (mm3)
DAY
Treatment (i.v.)

Fig. 11

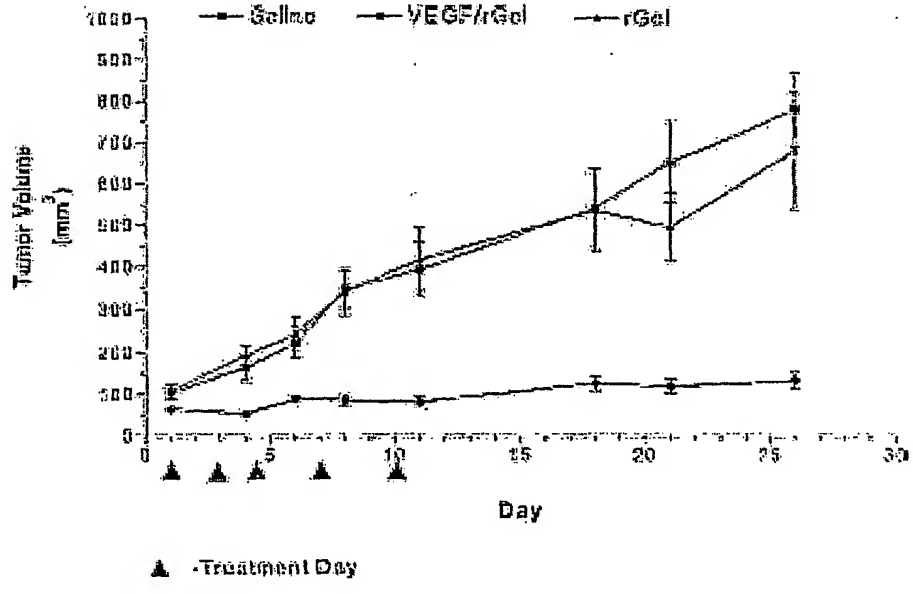
Gelmo
VEGF/rGel
rGel
Tumor Volume (mm3)
Day
Treatment Day

Fig. 12

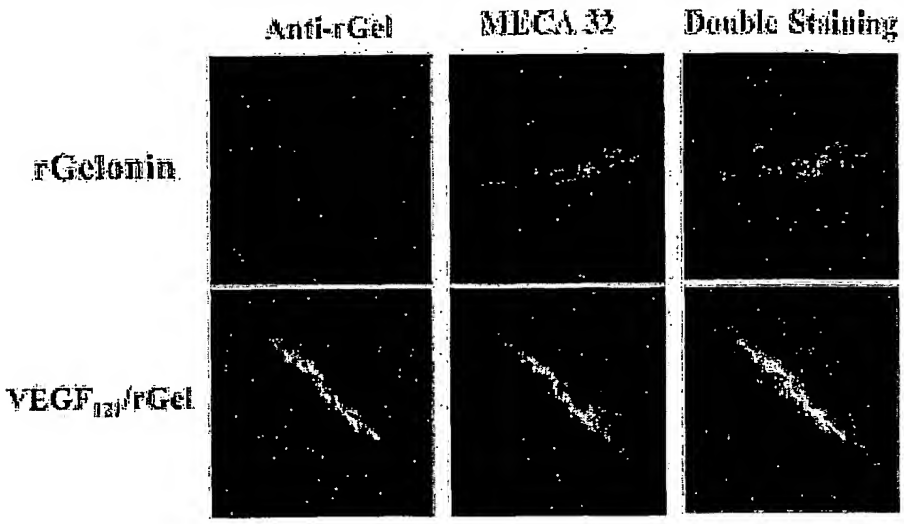
Anti-rGel
MECA 32
Double Staining
rGelonin
VEGF121/rGel

Fig. 13

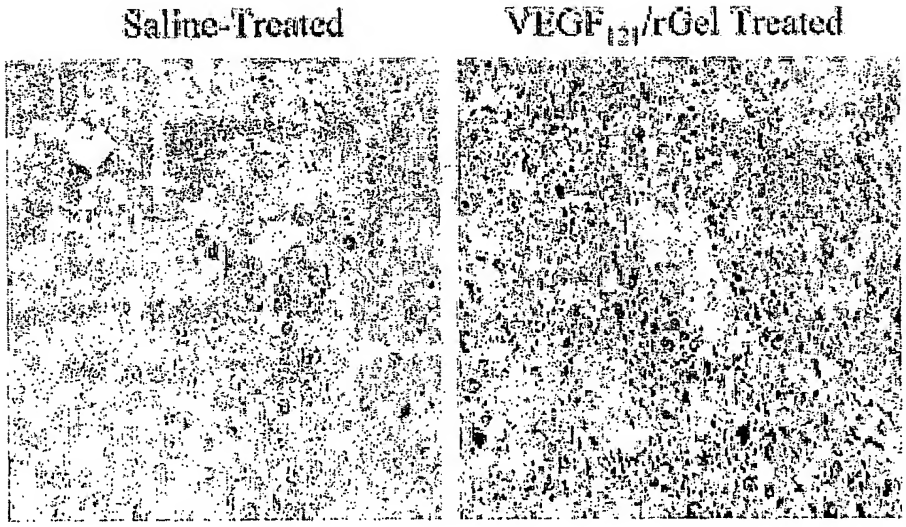
Saline-Treated
VEGF121/rGel Treated

Fig. 14

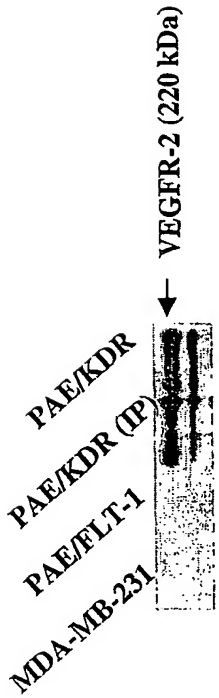

Fig. 15A

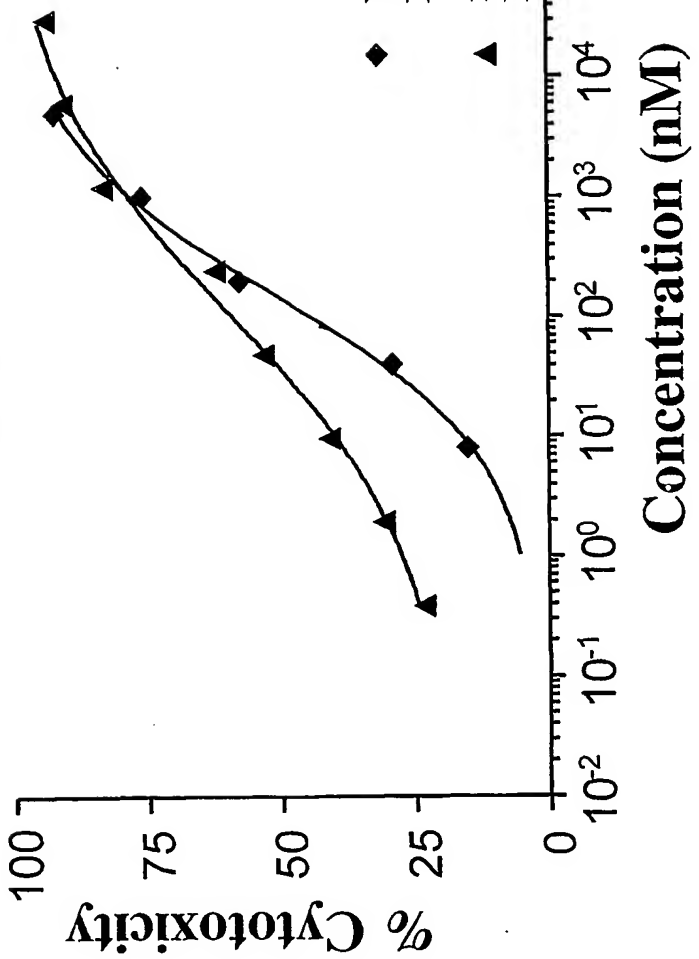

Fig. 15B

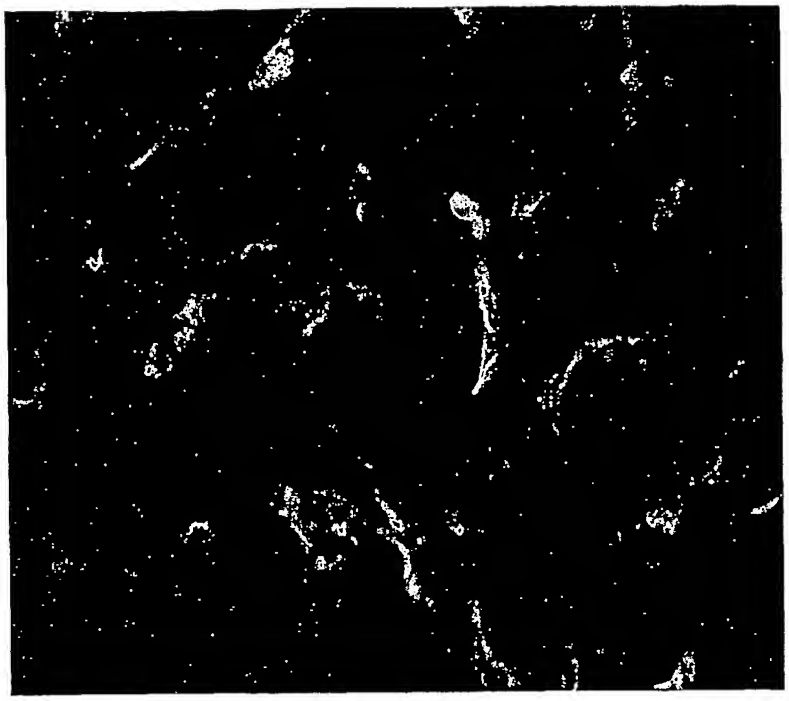

Fig. 16

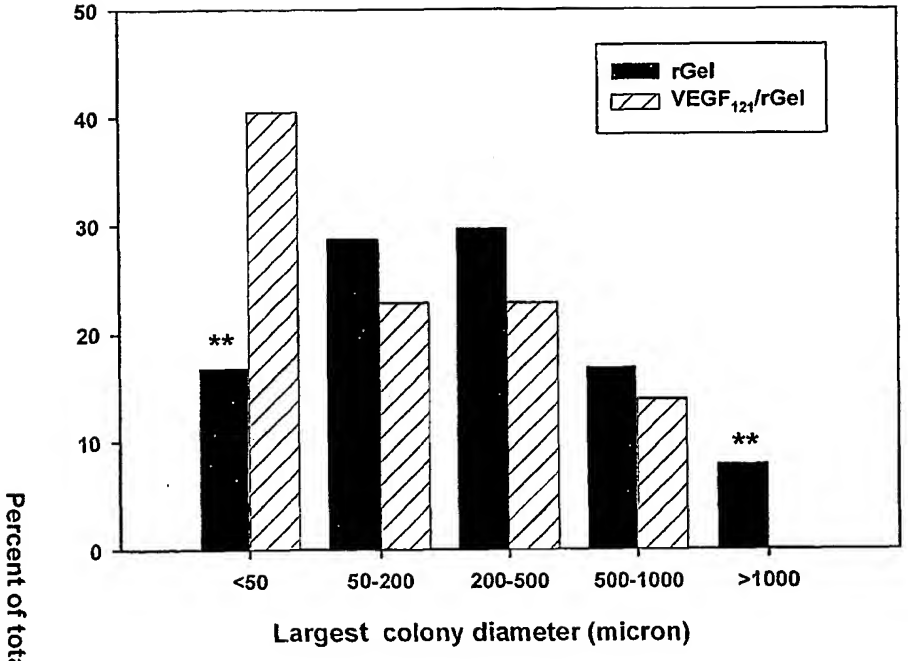
50
40
30
20
10
0
rGel
VEGF121/rGel
**
**
<50
50-200
200-500
500-1000
>1000
Largest colony diameter (micron)
Percent of total analyzed c

Fig. 17

Fig. 18A

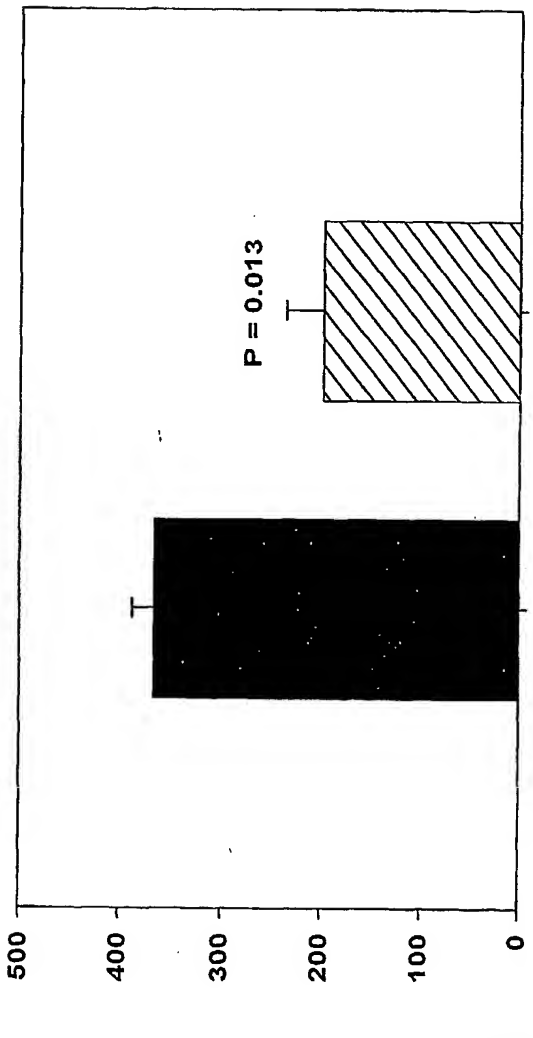

Fig. 18B

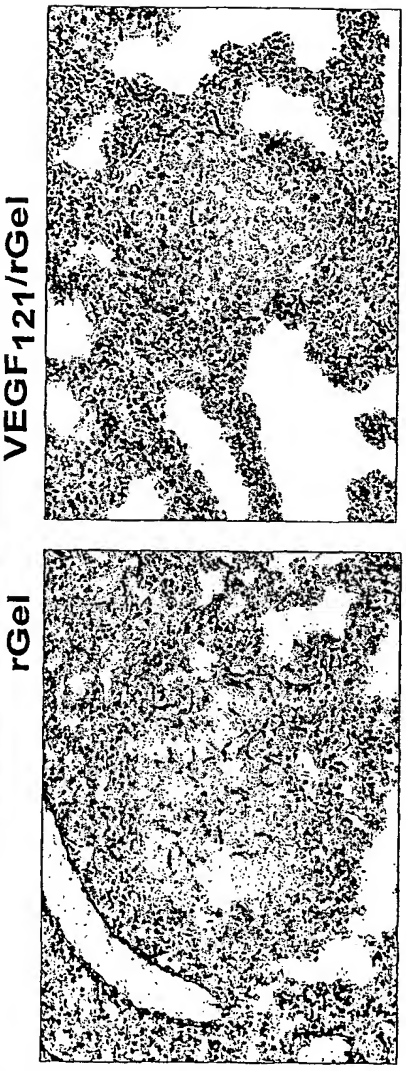

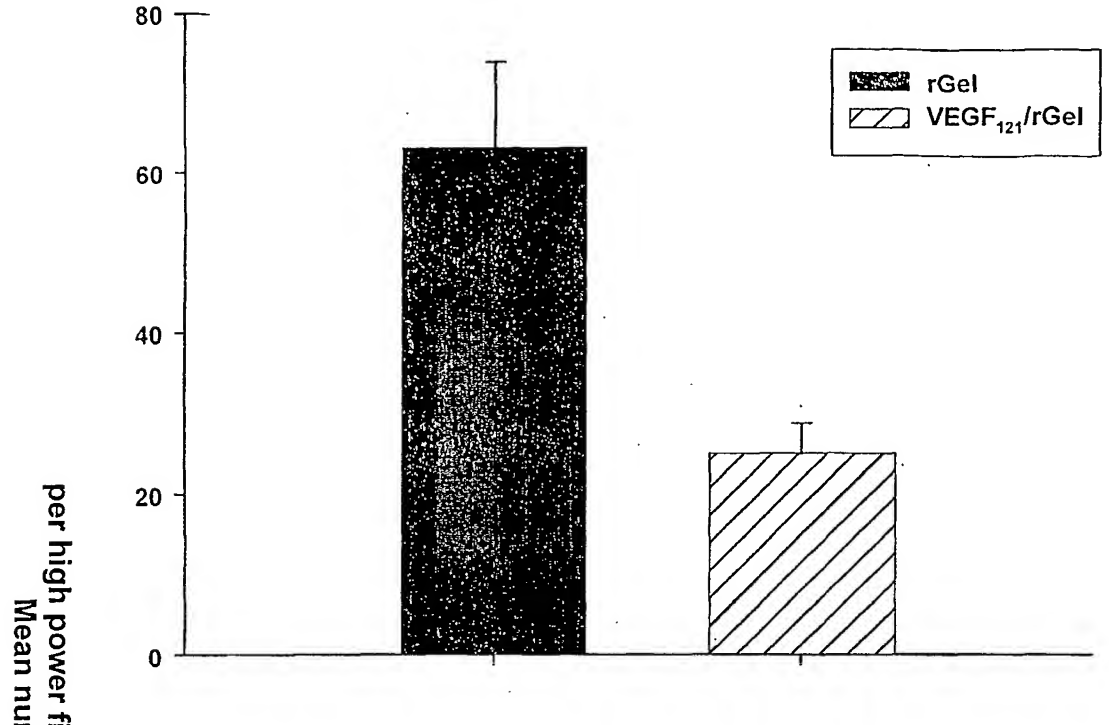
80
60
40
20
0
rGel
VEGF121/rGel
Mean number of Ki-67 labeled cells per high power field

Fig. 19

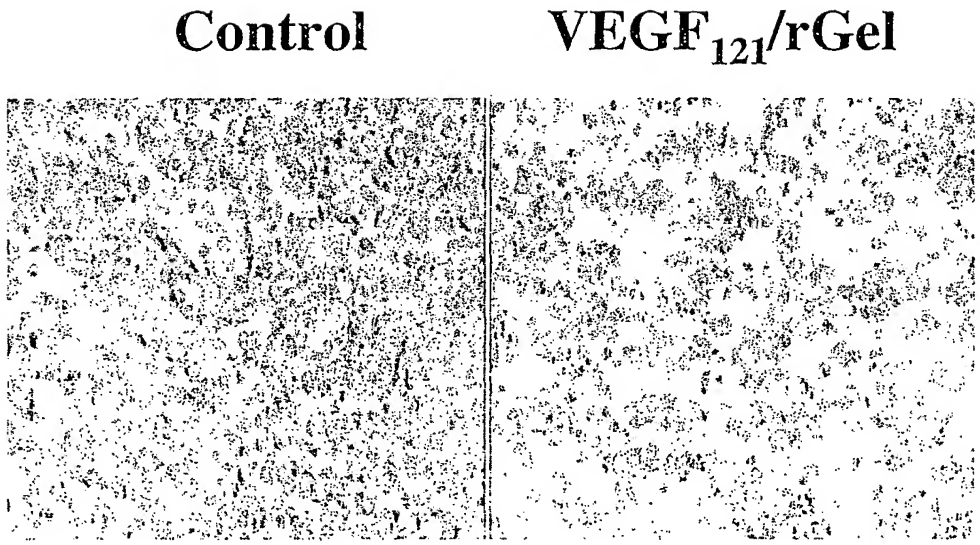
Control
VEGF121/rGel

Fig. 20

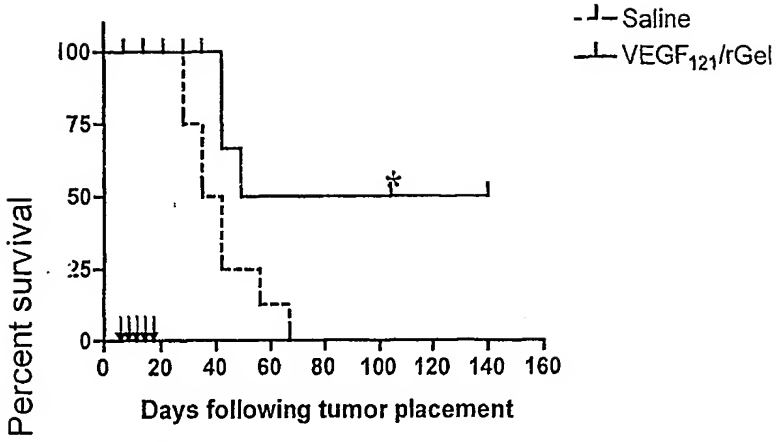

↓ Treatment days

* One mouse did not recover from anesthesia (no tumor)

Fig. 21

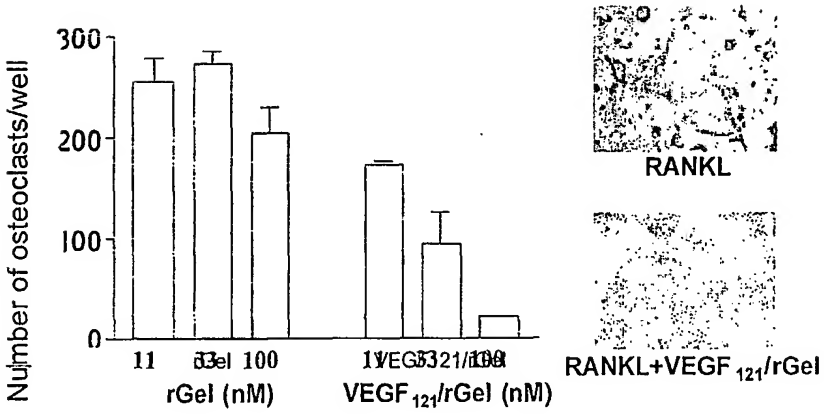

Fig. 22

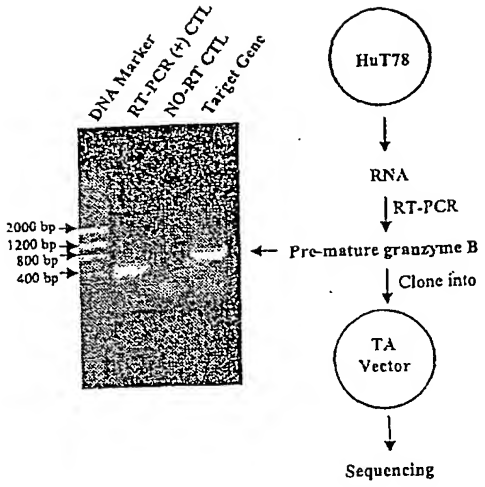


```
1/1                                                                  54/18
ATG CAA CCA ATC CTG CTT CTG CTG GCC TTC CTC CTG CTG CCC AGG GCA GAT GCA
  M   Q   P   I   L   L   L   L   A   F   L   L   L   P   R   A   G   A
                                                                     108/36
55/19
GGG GAG ATC ATC GGG GGA CAT GAG GCC AAG CCC CAC TCC CGC CCC TAC ATG GCT
  G   K   I   I   G   G   H   K   A   K   P   H   S   R   P   Y   M   A
                                                                     162/54
109/37
TAT CTT ATG ATC TGG GAT CAG AAG TCT CTG AAG AGG TGC GGT GGC TTC CTG ATA
  Y   L   M   I   W   D   Q   K   S   L   K   R   C   G   G   F   L   I
                                                                     216/72
163/55
CAA GAC GAC TTC GTG CTG ACA GCT GCT CAC TGT TGG GGA AGC TCC ATA AAT GTC
  Q   D   D   F   V   L   T   A   A   H   C   W   G   S   S   I   N   V
                                                                     270/90
217/73
ACC TTG GGG GCC CAC AAT ATC AAA GAA CAG GAG CCG ACC CAG CAG TTT ATC CCT
  T   L   G   A   H   N   I   K   K   Q   K   P   T   Q   Q   F   I   P
                                                                     324/108
271/91
GTG AAA AGA CCC ATC CCC CAT CCA GCC TAT AAT CCT AAG AAC TTC TCC AAC GAC
  V   K   R   P   I   P   H   P   A   Y   N   P   K   N   F   S   N   D
                                                                     378/126
325/109
ATC ATG CTA CTG CAG CTG GAG AGA AAG GCC AAG CGG ACC AGA GCT GTG CAG CCC
  I   M   L   L   Q   L   K   R   K   A   K   R   T   R   A   V   Q   P
                                                                     432/144
379/127
CTC AGG CTA CCT AGC AAC AAG GCC CAG GTG AAG CCA GGG CAG ACA TGC AGT GTG
  L   R   L   P   S   N   K   A   Q   V   K   P   G   Q   T   C   S   V
                                                                     486/162
433/145
GCC GGC TGG GGG CAG ACG GCC CCC CTG GGA AAA CAC TCA CAC ACA CTA CAA GAG
  A   G   W   G   Q   T   A   P   L   G   K   H   S   H   T   L   Q   E
                                                                     540/180
487/163
GTG AAG ATG ACA GTG CAG GAA GAT CGA AAG TGC GAA TCT GAC TTA CGC CAT TAT
  V   K   M   T   V   Q   E   D   R   K   C   E   S   D   L   R   H   Y
                                                                     594/198
541/181
TAC GAC AGT ACC ATT GAG TTG TGC GTG GGG GAC CCA GAG ATT AAA AAG ACT TCC
  Y   D   S   T   I   E   L   C   V   G   D   P   E   I   K   K   T   S
                                                                     648/216
595/199
TTT AAG GGG GAC TCT GGA GGC CCT CTT GTG TGT AAC AAG GTG GCC CAG GGC ATT
  F   K   G   D   S   G   G   P   L   V   C   N   K   V   A   Q   G   I
                                                                     702/234
649/217
GTC TCC TAT GGA CGA AAC AAT GGC ATG CCT CCA CGA GCC TGC ACC AAA GTC
  V   S   Y   G   R   N   N   G   M   P   P   R   A   C   T   K   V
                                                                     744/248
703/235
TCA AGC TTT GTA CAC TGG ATA AAG AAA ACC ATG AAA CGC TAC TAA (SEQ ID NO: 14)
  S   S   F   V   H   W   I   K   K   T   M   K   R   Y   -  (SEQ ID NO:15)
```

Fig. 23

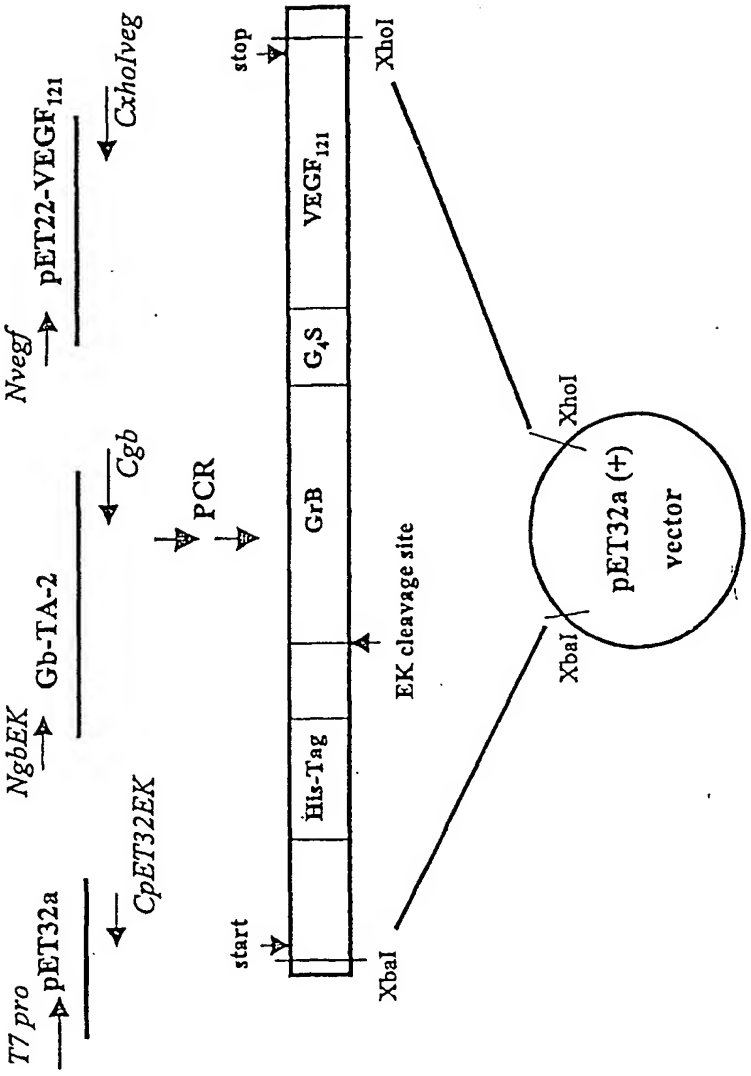
T7 pro
pET32a
CpET32EK
NgbEK
Gb-TA-2
Cgb
PCR
Nvegf
pET22-VEGF121
CxhoIveg
start
His-Tag
GrB
EK cleavage site
G4S
VEGF121
stop
XbaI
XhoI
XbaI
XhoI
pET32a (+)
vector

Fig. 24

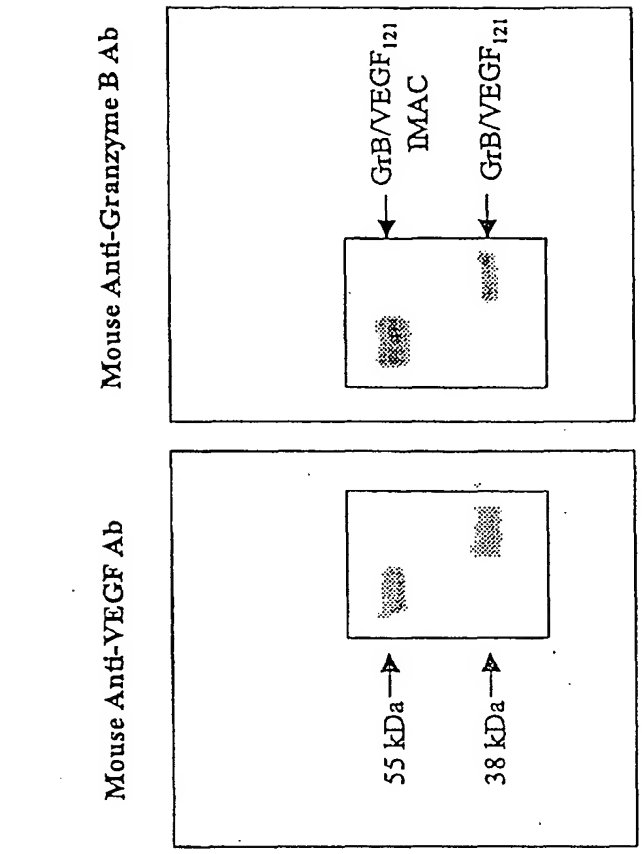

Fig. 25B

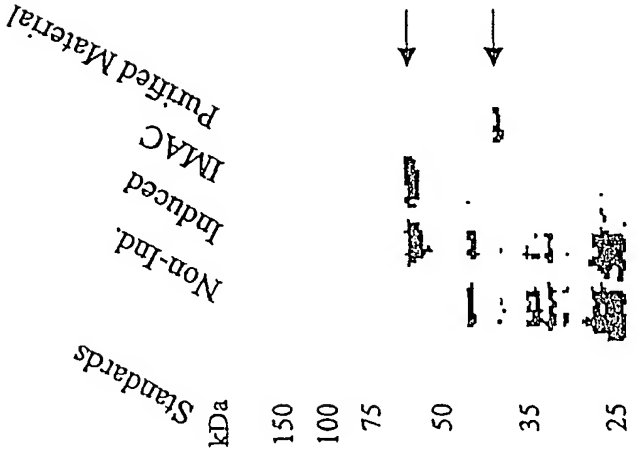

Fig. 25A

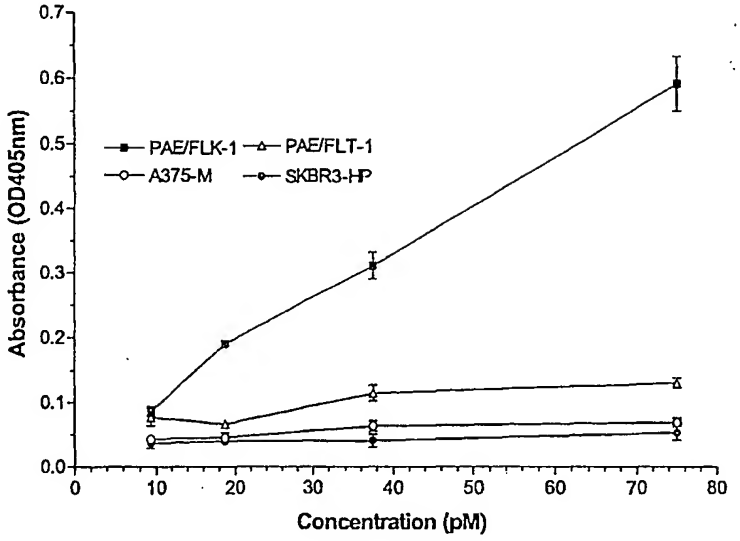

Fig. 26A

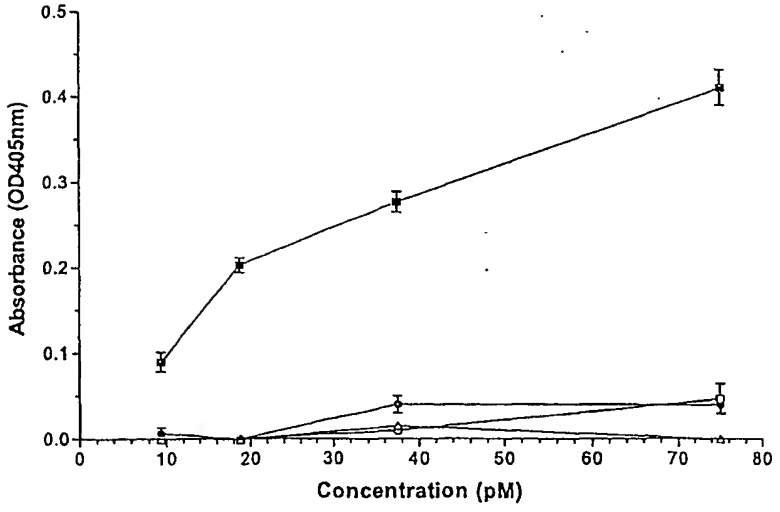

Fig. 26B

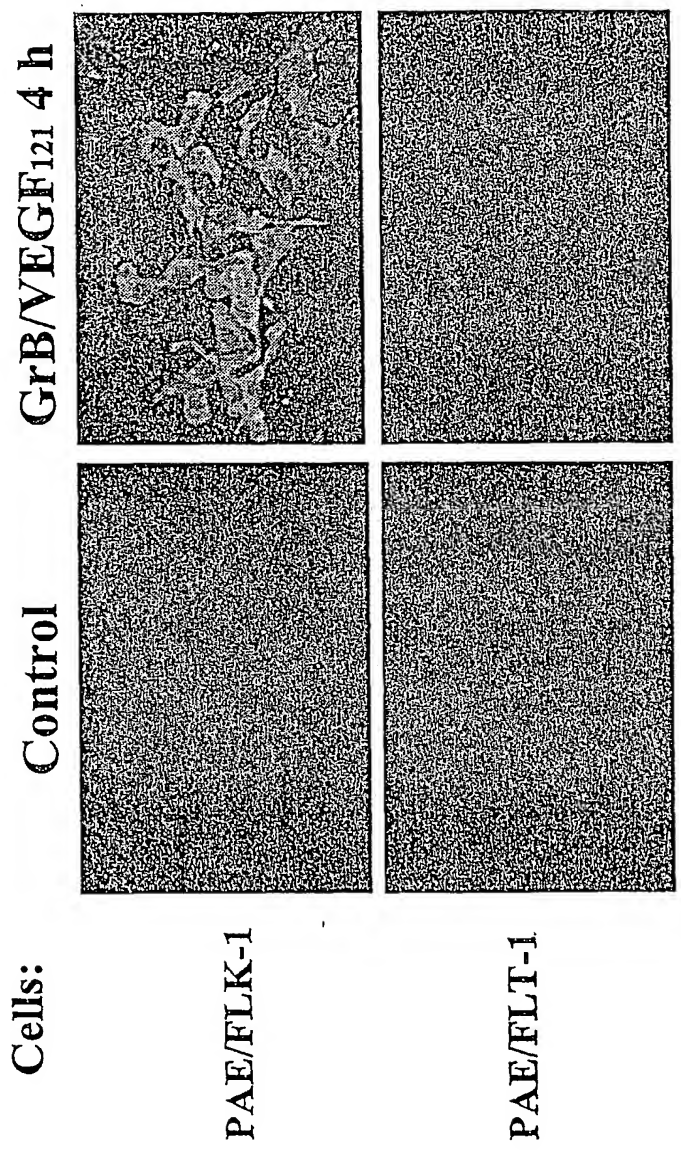

Fig. 27

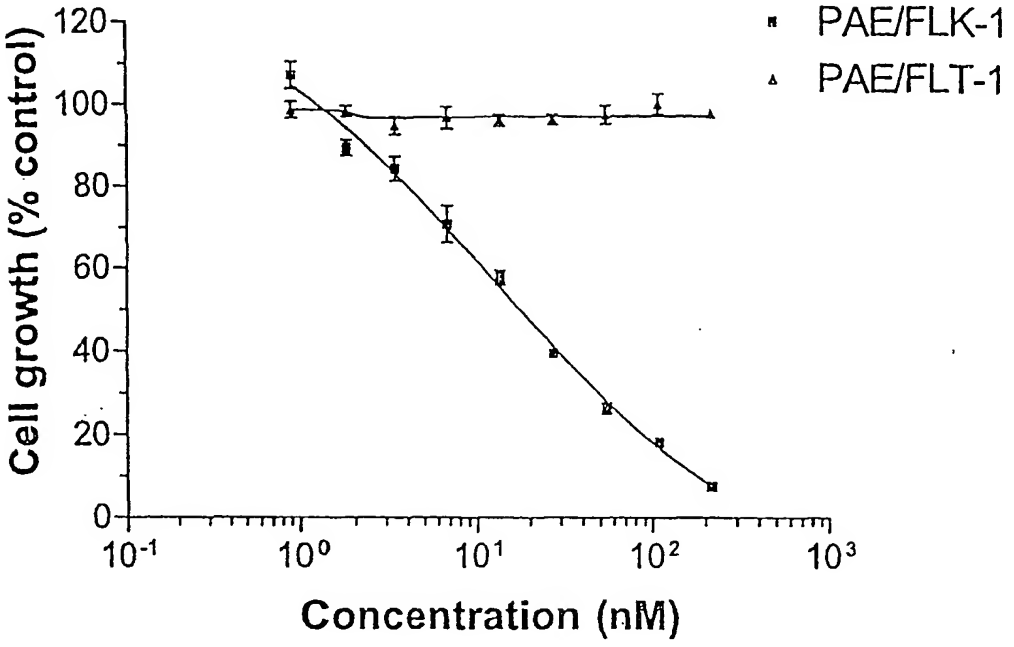

Fig. 28A

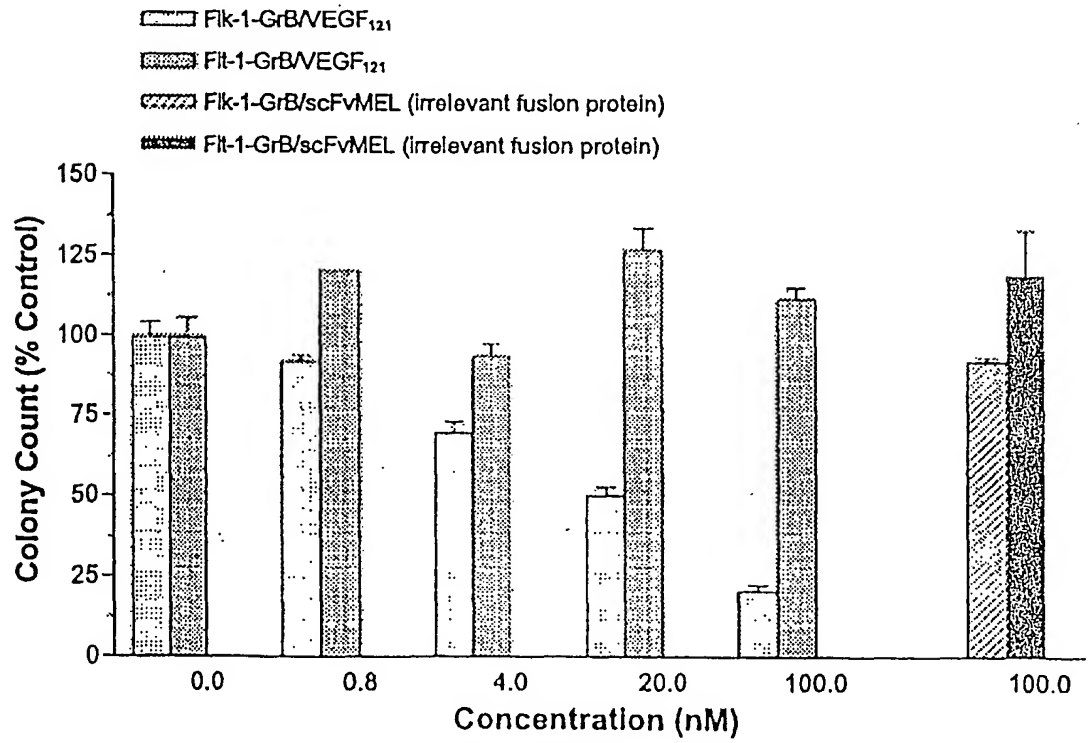

Fig. 28B

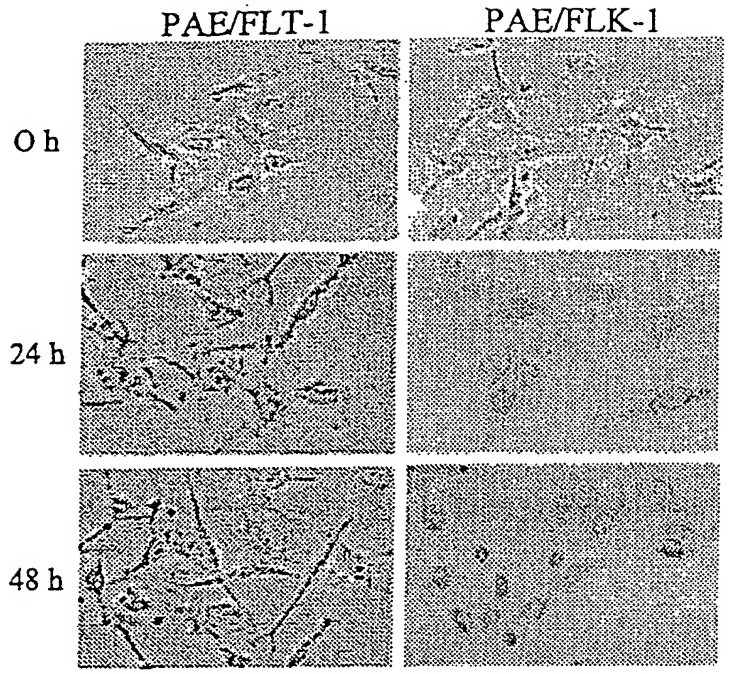

Fig. 29A

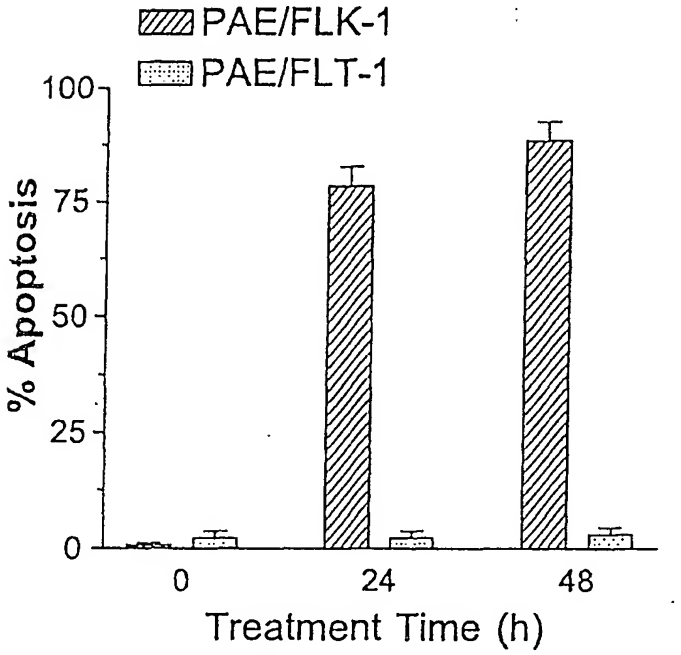

Fig. 29B

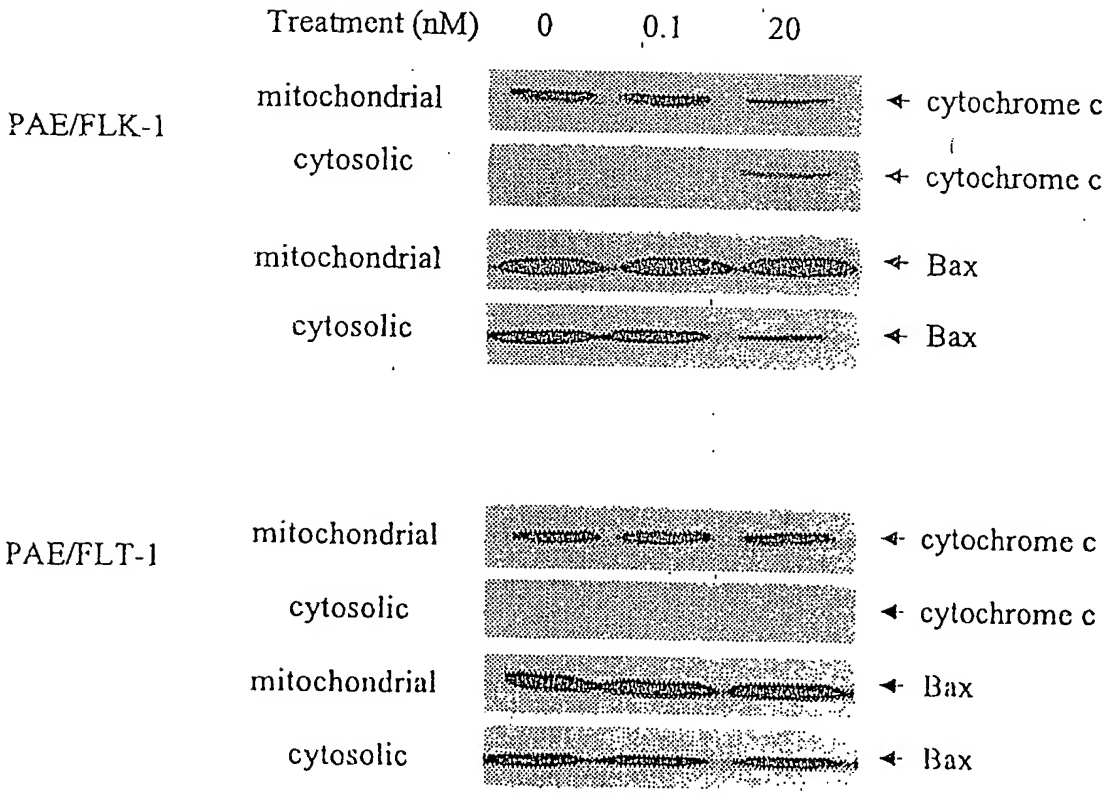
Treatment (nM) 0 0.1 20
PAE/FLK-1
mitochondrial
cytosolic
mitochondrial
cytosolic
cytochrome c
cytochrome c
Bax
Bax
PAE/FLT-1
mitochondrial
cytosolic
mitochondrial
cytosolic
cytochrome c
cytochrome c
Bax
Bax

Fig. 30

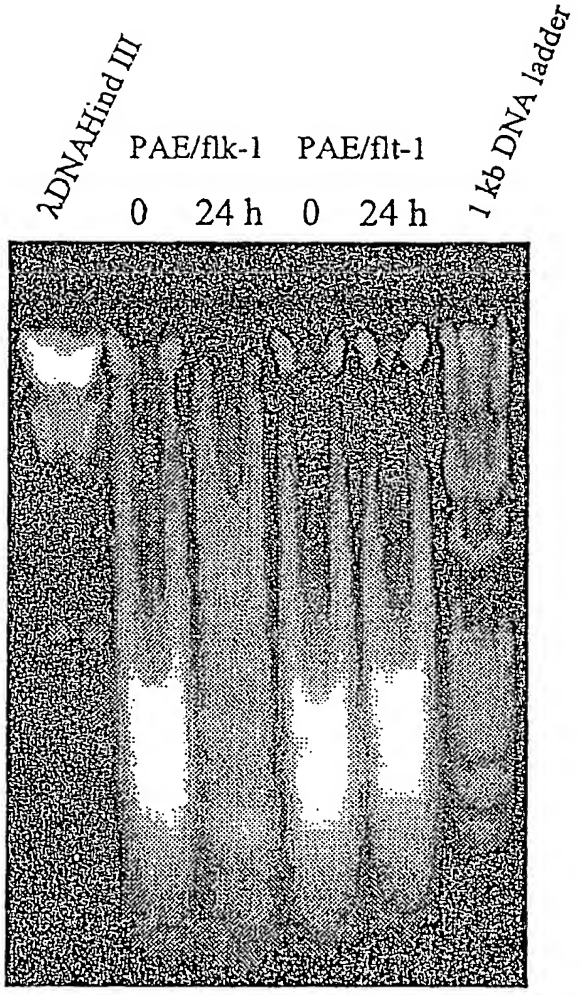

Fig. 31

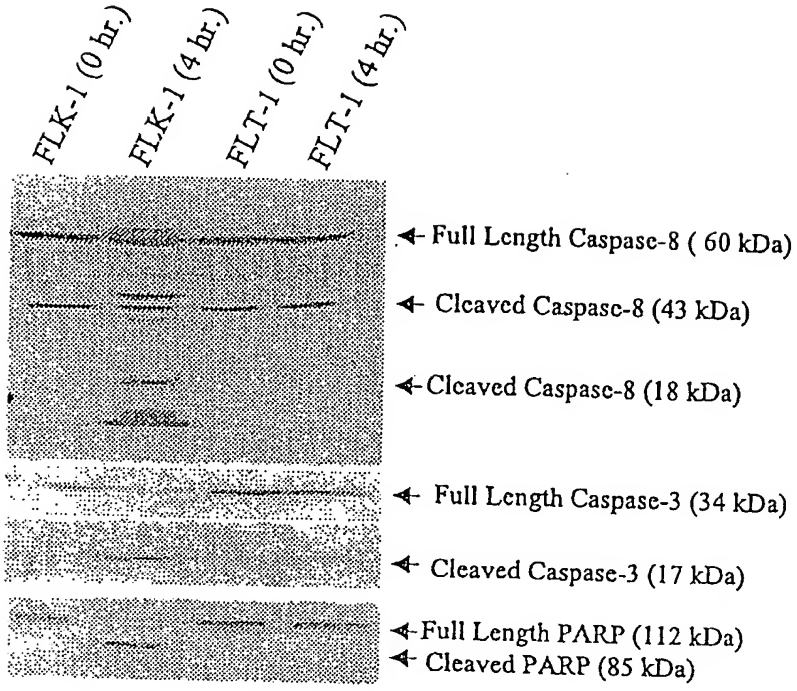
FLK-1 (0 hr.)
FLK-1 (4 hr.)
FLT-1 (0 hr.)
FLT-1 (4 hr.)
Full Length Caspase-8 (60 kDa)
Cleaved Caspase-8 (43 kDa)
Cleaved Caspase-8 (18 kDa)
Full Length Caspase-3 (34 kDa)
Cleaved Caspase-3 (17 kDa)
Full Length PARP (112 kDa)
Cleaved PARP (85 kDa)

Fig. 32

SEQUENCE LISTING

<110> Research Development Foundation

<120> Vascular Endothelial Growth Factor Fusion Constructs And Uses Thereof

<130> D6519PCT

<141> 2004-05-14

<150> 60/476,209
<151> 2003-06-05

<160> 15

<210> 1
<211> 33
<212> DNA
<213> Artificial Sequence

<220>
<221> primer_bind
<223> primer VEGF Nterm

<400> 1
tggtcccagg ctcatatggc acccatggca gaa 33

<210> 2
<211> 38
<212> DNA
<213> Artificial Sequence

<220>
<221> primer_bind
<223> primer VEGF Cterm

<400> 2
tctagaccgg agccaccgcc accccgcctc ggcttgtc 38

<210> 3

<211> 33
<212> DNA
<213> Artificial Sequence

<220>
<221> primer_bind
<223> primer Gel Nterm

<400> 3
ggtggcggtg gctccggtct agacaccgtg agc 33

<210> 4
<211> 45
<212> DNA
<213> Artificial Sequence

<220>
<221> primer_bind
<223> primer Gel Cterm

<400> 4
aaggctcgtg tcgacctcga gtcattaagc tttaggatct ttatc 45

<210> 5
<211> 36
<212> DNA
<213> Artificial Sequence

<220>
<221> primer_bind
<223> primer NcoIgb

<400> 5
ggtggcggtg gctccatgga accaatcctg cttctg 36

<210> 6
<211> 39
<212> DNA
<213> Artificial Sequence

<220>

<221> primer_bind
<223> primer CxhoIgb

<400> 6
gccaccgcct ccctcgagct attagtagcg tttcatggt 39

<210> 7
<211> 5
<212> PRT
<213> Artificial Sequence

<220>
<221> DOMAIN
<223> a cleavage site for EK

<400> 7
Asp Asp Asp Asp Lys
5

<210> 8
<211> 39
<212> DNA
<213> Artificial Sequence

<220>
<221> primer_bind
<223> primer NgbEK

<400> 8
ggtaccgacg acgacgacaa gatcatcggg ggacatgag 39

<210> 9
<211> 30
<212> DNA
<213> Artificial Sequence

<220>
<221> primer_bind
<223> primer Cgb

<400> 9

ggagccaccg ccaccgtagc gtttcatggt 30

<210> 10
<211> 30
<212> DNA
<213> Artificial Sequence

<220>
<221> primer_bind
<223> primer Nvegf

<400> 10
ggtggcggtg gctccgcacc catggcagaa 30

<210> 11
<211> 42
<212> DNA
<213> Artificial Sequence

<220>
<221> primer_bind
<223> primer CxhoI veg

<400> 11
aaggctcgtg tcgacctcga gtcattaccg cctcggcttg tc 42

<210> 12
<211> 18
<212> DNA
<213> Artificial Sequence

<220>
<221> primer_bind
<223> primer T7 promoter

<400> 12
taatacgact cactatag 18

<210> 13
<211> 30

<212> DNA
<213> Artificial Sequence

<220>
<221> primer_bind
<223> primer CpET32EK

<400> 13
cttgtcgtcg tcgtcggtac ccagatctgg 30

<210> 14
<211> 744
<212> DNA
<213> *Homo sapiens*

<220>
<221> gene
<223> human granzyme B with signal peptide sequence

<400> 14
atgcaaccaa tcctgcttct gctggccttc ctcctgctgc ccagggcaga 50
tgcaggggag atcatcgggg gacatgaggc caagccccac tcccgccct 100
acatggctta tcttatgatc tgggatcaga agtctctgaa gaggtgcggt 150
ggcttcctga tacaagacga cttcgtgctg acagctgctc actgttgggg 200
aagctccata aatgtcacct tgggggccca caatatcaaa gaacaggagc 250
cgacccagca gtttatccct gtgaaaagac ccatccccca tccagcctat 300
aatcctaaga acttctccaa cgacatcatg ctactgcagc tggagagaaa 350
ggccaagcgg accagagctg tgcagccct caggctacct agcaacaagg 400
cccaggtgaa gccagggcag acatgcagtg tggccggctg ggggcagacg 450
gccccctgg gaaaacactc acacacacta caagaggtga agatgacagt 500
gcaggaagat cgaaagtgcg aatctgactt acgccattat tacgacagta 550
ccattgagtt gtgcgtgggg gacccagaga ttaaaaagac ttcctttaag 600
ggggactctg gaggccctct tgtgtgtaac aaggtggccc agggcattgt 650
ctcctatgga cgaaacaatg gcatgcctcc acgagcctgc accaaagtct 700
caagctttgt acactggata aagaaaacca tgaaacgcta ctaa 744

<210> 15
<211> 247
<212> PRT
<213> *Homo sapiens*

<220>

<221> PROPEP
<223> human granzyme B with signal peptide sequence

<400> 15

```
Met Gln Pro Ile Leu Leu Leu Leu Ala Phe Leu Leu Leu Pro Arg
 1               5                  10                  15
Ala Gly Ala Gly Glu Ile Ile Gly Gly His Glu Ala Lys Pro His
            20                  25                  30
Ser Arg Pro Tyr Met Ala Tyr Leu Met Ile Trp Asp Gln Lys Ser
        35                  40                  45
Leu Lys Arg Cys Gly Gly Phe Leu Ile Gln Asp Asp Phe Val Leu
    50                  55                  60
Thr Ala Ala His Cys Trp Gly Ser Ser Ile Asn Val Thr Leu Gly
65                  70                  75
Ala His Asn Ile Lys Glu Gln Glu Pro Thr Gln Gln Phe Ile Pro
                80                  85                  90
Val Lys Arg Pro Ile Pro His Pro Ala Tyr Asn Pro Lys Asn Phe
            95                  100                 105
Ser Asn Asp Ile Met Leu Leu Gln Leu Glu Arg Lys Ala Lys Arg
        110                 115                 120
Thr Arg Ala Val Gln Pro Leu Arg Leu Pro Ser Asn Lys Ala Gln
    125                 130                 135
Val Lys Pro Gly Gln Thr Cys Ser Val Ala Gly Trp Gly Gln Thr
140                 145                 150
Ala Pro Leu Gly Lys His Ser His Thr Leu Gln Glu Val Lys Met
155                 160                 165
Thr Val Gln Glu Asp Arg Lys Cys Glu Ser Asp Leu Arg His Tyr
            170                 175                 180
Tyr Asp Ser Thr Ile Glu Leu Cys Val Gly Asp Pro Glu Ile Lys
        185                 190                 195
Lys Thr Ser Phe Lys Gly Asp Ser Gly Gly Pro Leu Val Cys Asn
    200                 205                 210
Lys Val Ala Gln Gly Ile Val Ser Tyr Gly Arg Asn Asn Gly Met
215                 220                 225
Pro Pro Arg Ala Cys Thr Lys Val Ser Ser Phe Val His Trp Ile
            230                 235                 240
Lys Lys Thr Met Lys Arg Tyr
        245
```